

82-#855-#10917

9

GEOLOGY, GEOCHRONOLOGY AND
LITHOGEOCHEMISTRY OF
MINERALIZATION AND ALTERATION
BJ GROUPS 1 AND 2

LIARD MINING DIVISION
104 G/2W
57°08'N, 130°58'W

OWNED BY **GEOLOGICAL BRANCH**
TECK CORPORATION **ASSESSMENT REPORT**

OPERATED BY
TECK EXPLORATIONS LTD.

10,917

PETER HOLBECK, B.Sc.
Vancouver, B. C.

December 1982

TABLE OF CONTENTS

	<u>Page</u>
1. Introduction	
1.1 Location and Access	1
1.2 Property and History	1
1.3 Climate and Physiography	5
1.4 Work Done	5
2. Geology	
2.1 Regional Setting	6
2.2 Stratigraphy	6
2.3 Structure	8
2.4 Metamorphism	9
2.5 Geochronology	9
3. Litho geochemistry	
3.1 Methods	13
3.2 Major Element Chemistry	13
3.3 Trace Element Chemistry	19
4. Mineralization and Alteration	
4.1 Description of Mineralization	25
4.2 Sulphide Mineralogy	25
4.2.1 Mineralogy	28
4.2.2 Geothermometry and Paragenesis	33
4.3 Alteration Petrology	37
4.4 Genesis	40
5. Summary and Conclusions	42
References	44

LIST OF FIGURES

Figure 1.1 Location Map	2
1.2 Claim Map	4
2.1 Rb/Sr Isochrons	10
2.2 Summary of Regional Geochronology	12
3.1 Harker Variation Diagram	15
3.2 Alkalies-Silica Plot	16
3.3 AFM Diagram	17
3.4 K/Na vs Si/(Fc + Mg + Ca) Plot	18
3.5 Ti-Zr-Y Ternary Discrimination Diagram	22
3.6 Al-Ti-Zr Rates vs MgO Plot	23
4.1 Composite Line Diagram	35
4.2 Composite Vandeveer Diagram	36
4.3 Major Element Variation with Alteration	39

LIST OF TABLES AND APPENDICES

Table 1.1	Claim Data	3
3.1	Major Element Determinations	14
3.2	Trace Elements Determinations	21
Appendix I	Analytical Precision Chart	
II	Major Trace Element Correlation Diagram	
III	Sample Location (in pocket)	
IV	Statement of Costs	
V	Certificate of Qualifications	

1. INTRODUCTION

1.1 Location and Access

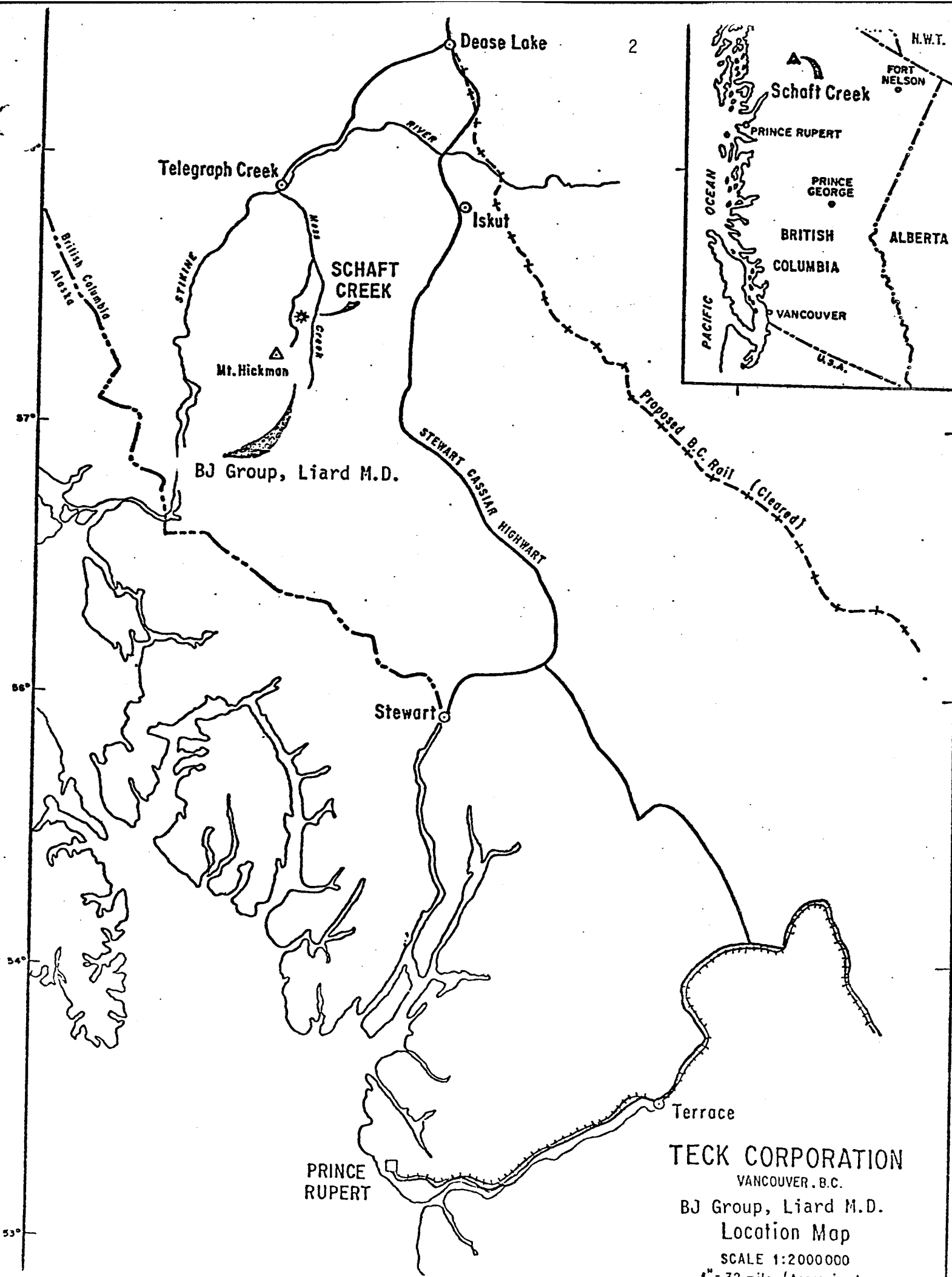
The BJ group and related claims are situated at the headwaters of Mess Creek, $57^{\circ}08'$ north, $130^{\circ}50'$ west, approximately 130 km southwest of Dease Lake, British Columbia. The area is covered by NTS map sheet 104 G/2W and lies within the Liard Mining Division.

Although the Stewart-Cassiar highway passes 50 km east of the property the nearest permanent settlement is Telegraph Creek, 60 km to the north. An airstrip served by Trans Provincial Airlines from Terrace is located at Teck's Schaft Creek deposit, 15 km northwest of the claims. Property access is by helicopter from Schaft Creek. Permanent helicopter bases are located at Dease Lake and Eddontenajon.

1.2 Property and History

The initial claims, BJ, Bee and Jay, were staked in July 1980 based on follow-up of stream geochemistry. Subsequent staking of Windy, Grey, Rainy and Day claims was completed in August of 1980. Very, Valley and Fall claims were recorded in September, 1980 but have since been reduced. Three additional claims, Snout, JB, and Wish were located in September, 1981. Claim data are summarized in Table 1.

Although indication of early prospecting on the property has been found, there is no record of any previous claims having been staked in the area.



<u>Name</u>	<u>Units</u>	<u>Date Located</u>	<u>Date Recorded</u>	<u>Record No.</u>
Bee	4	13 July 1980	29 July 1980	1478 (7)
Jay	20	16 July 1980	29 July 1980	1479 (7)
BJ	20	10 July 1980	29 July 1980	1480 (7)
Windy	18	20 Aug. 1980	29 Aug. 1980	1556 (8)
Grey	12	14 Aug. 1980	29 Aug. 1980	1557 (8)
Rainy	12	13 Aug. 1980	29 Aug. 1980	1558 (8)
Day	8	13 Aug. 1980	29 Aug. 1980	1559 (8)
Very	2	13 Aug. 1980	29 Aug. 1980	1555 (8)
Fall	2	Sep. 1980	22 Sep. 1980	1623 (9)
Valley	6	Sep. 1980	22 Sep. 1980	1626 (9)
JB	6	1 Sep. 1981	22 Sep. 1981	2064 (9)
Wish	2	1 Sep. 1981	22 Sep. 1981	2065 (9)
Snout	2	1 Sep. 1981	22 Sep. 1981	2066 (9)
TOTAL UNITS	= 114			

TABLE 1: SUMMARY OF CLAIM DATA, BJ GROUP AND RELATED GROUPS

TO EAST SEE MAP 104G/3E

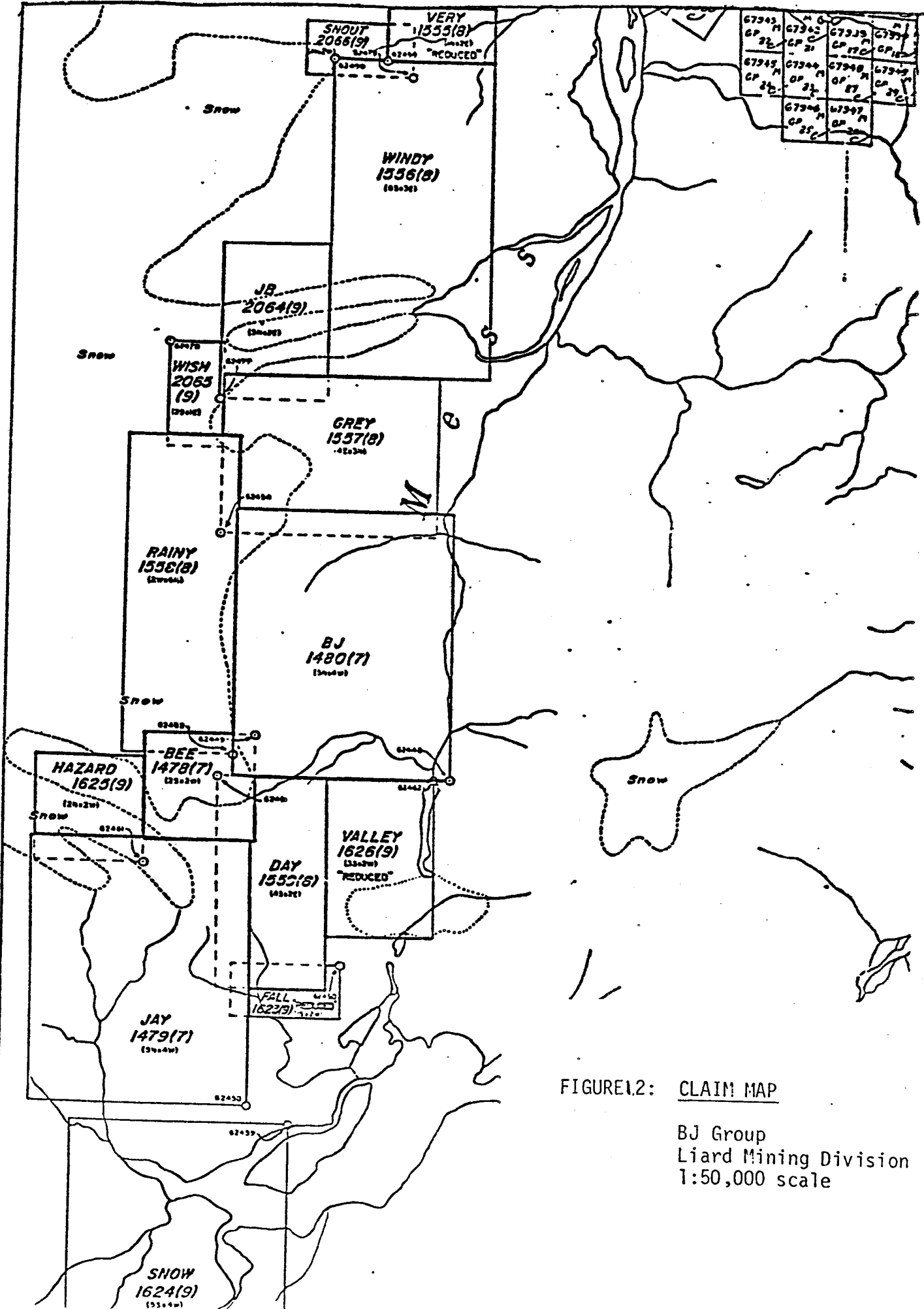


FIGURE 1.2: CLAIM MAP

BJ Group
Liard Mining Division
1:50,000 scale

1.3 Climate and Physiography

Located on the eastern flank of the Coast Mountains, the area is rugged with elevations ranging from 1,000 to 2,000 m. The property is bounded to the south and west by ice fields and to the north and east by the Mess Creek valley. Numerous alpine glaciers transect the property exploiting zones of structural weakness and providing good outcrop exposure in areas of recent retreat.

The climate is cool and moist resulting in snow cover for nine months of the year. Moderate precipitation and topography have combined to produce rapid erosion within the area.

1.4 Work Done

During the winter of 1981-82, rocks collected from BJ groups 1 and 2 were analyzed in detail as part of M.Sc. thesis research at the University of British Columbia. Details of mineralization and alteration were investigated utilizing both conventional microscopy and scanning electron microscopy on 40 polished thin sections. An additional 18, 2 x 5 cm polished sections were studied by reflected light techniques for textural and paragenetic relationships. Sixty-four samples, including field and laboratory duplicates, were analyzed by x-ray fluorescence for major and trace elements.

Thirteen Rb-Sr determinations and one K-Ar determination provided ages of mineralization and alteration.

2. GEOLOGY

2.1 Regional Setting

The area of study is underlain by mid-to late-Paleozoic, polydeformed and metamorphosed volcanics, volcani-clastics, and sediments typical of eugeoclinal sequences. All pre-Triassic rocks in the area are grouped in the Stikine Assemblage: an allochthonous ocean island terrain accreted to North America in mid to late Mesozoic time (Monger, 1981; 1977).

To the north and west, the area is unconformably overlain by Upper Triassic shales, chert, sandstone and conglomerates. These sediments are unmetamorphosed, only slightly deformed and bounded to the west by Coast Range intrusives. To the south and east, the property is in fault contact with lesser deformed and metamorphosed Permian and/or Triassic fragmental volcanics.

2.2 Stratigraphy

Facies changes, complex interfolding and alteration within the property area severely complicate stratigraphic contacts and succession within the Paleozoic rocks. On the basis of composition and texture a number of subdivisions can be made. In structural sequence from upper to lower they are:

- 1) Unit 5, GRST. - foliated to massive; fine to coarse grained greenstones. Probably gabbro sills.

- 2) Unit 4, FVCS. - fine to coarse felsic tuff and/or breccia.
Generally minor to severe alteration, occasionally mylonitized.
- 3) Unit 3, PGST. - Intercalated purple and green, mafic phylonites.
Some exposures display fragmental textures. Rare limestone lenses near top of the section.
- 4) Unit 2, CHST. - massive chlorite schist and chlorite phylonite.
In part, equivalent to Unit 3, and as small lenses in Unit 1.
- 5) Unit 1, ARGL. - Argillaceous to graphitic schist.

Folding and thrust faulting causes partial repeats and/or reversals of the sequence over much of the property. In addition, two non-stratigraphic alteration units also occur:

- 1) Unit A, QMCS - quartz, muscovite (± chrome), carbonate, ± talc schist.
- 2) Unit B, CALT - hemitized, carbonate alteration zones through to large fault fillings of botryoidal and brecciated carbonate.

Unit A appears to be an alteration product of all units but is primarily derived from either unit 4 or, possibly, an unknown parent. Unit B is a late feature that is mostly fracture controlled, but occasionally stratabound. Both units are spatially associated with mineralization.

2.3 Structure

Four distinct phases of folding are evident. Two early phases of isoclinal folding have colinear fold axes, trending north, northwest. Axial planes were nearly perpendicular resulting in crenulation cleavage and Ramsey type 2 interference patterns. Metamorphism and metasomatism took place prior to the onset of the second deformational phase. The extreme ductility contrast between lithologies resulted in most of the strain being taken by units 4 and A.

The third phase of folding is related to north-south compression and has produced kinkbanding, chevron folds and broad open warps in well developed foliation. It is likely that this phase was coincident with north-south strike slip faulting.

A final phase of east-west compressional stress produced a northeasterly trending, vertical, open fold which flattens to the north. This phase dramatically intensifies to the west, where upright tight folds with amplitudes of 1 km can be seen. The great variation of fold style over short distances during this phase was probably due to forceful emplacement of plutonic rocks.

2.4 Metamorphism

Variable proportions of albite, chlorite, quartz and epidote form the dominant mineral assemblage, which is compatible with greenschist facies metamorphism. Most metamorphic minerals were formed during or before the first phase of deformation. A post tectonic assemblage of tremolite + quartz + calcite is stable at temperatures of between 490°C and 540°C (depending on CO₂ content of fluid phase) at 1000 bars pressure (Winkler, 1976) and indicates a late metamorphic stage. Late metamorphism is indicated in other areas by the formation of post kinematic biotite. Metamorphic overprinting appears to be localized in areas of late stage mineralization.

2.5 Geochronology

Thirteen whole rock Rb-Sr age determinations were carried out both on altered and unaltered rocks collected from various localities on the property. A single K/Ar age was obtained from Cr-muscovite associated with mineralization. All age determinations were performed in the geochronology labs at U.B.C. Rb-Sr samples and their isochrons are shown on Figure 2-1. Sample locations are given on the map in Appendix 3.

Under normal conditions, Rb-Sr determinations on mineral separates yield metamorphic ages and whole rock determinations give original rock age. Highly altered or metasomatized rocks, as is the case here, yield metamorphic/metasomatic ages due to complete re-equilibration of ⁸⁷Sr:⁸⁶Sr ratios. An isochron calculated by computer using the York technique of least squares regression for all data (see table 2-1) gives an age of 201±16 Ma. Figure 2-1 shows isochrons plotted for data

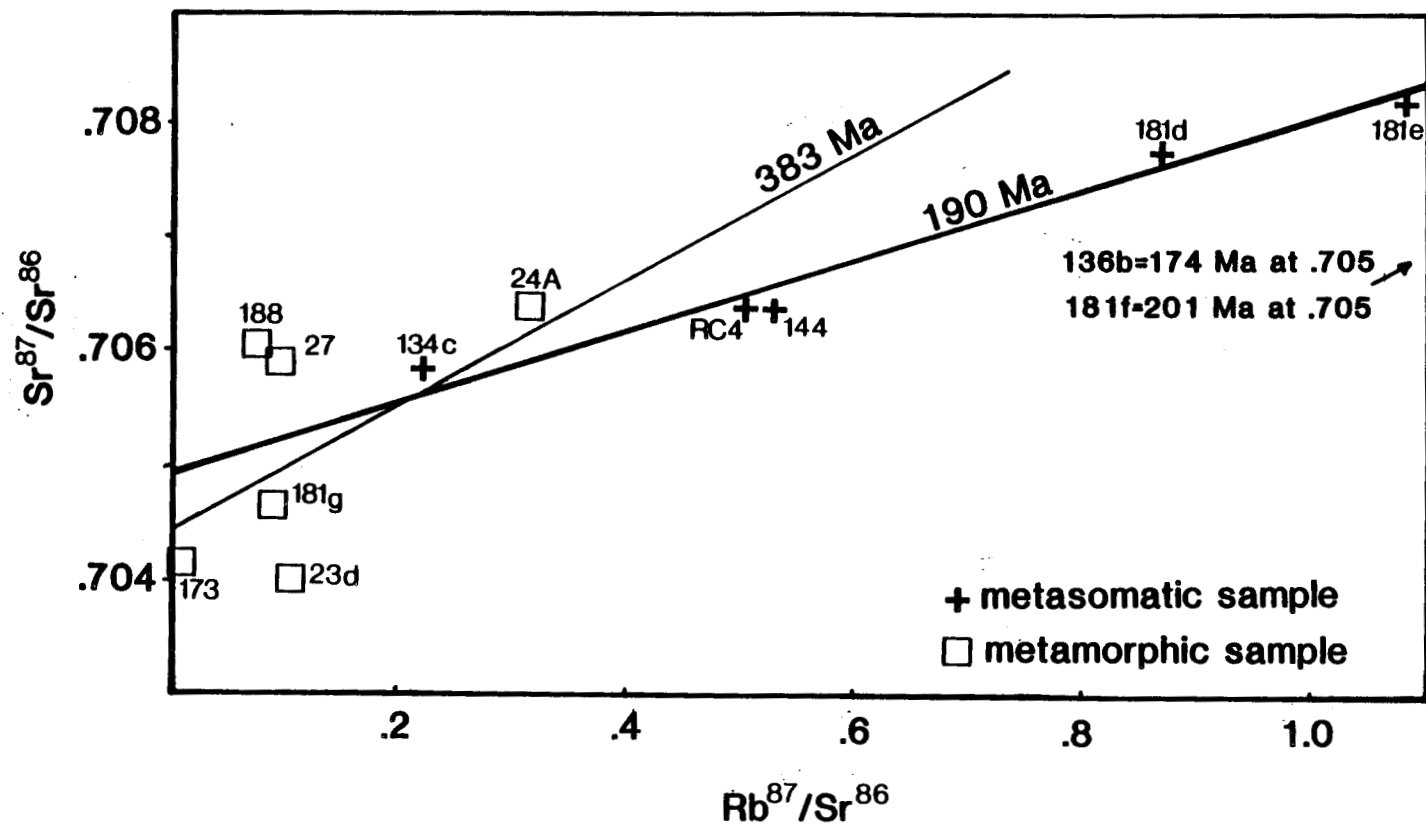


Figure 2.1: Rubidium-strontium isochrons for metasomatic and metamorphic samples. Metasomatic isochron of 190±11 Ma is concordant with K/Ar data. Unaltered samples fail to define a significant isochron but trend towards an increase in age.

segregated into altered and unaltered samples on the basis of chemistry and petrography. Metasomatic samples have an isochron at 190 ± 11 Ma. Unaltered data show too much scatter to yield a significant age determination but trend towards an older age. Geological age constraints are provided by fossils. Overlying and structurally conformable limestone immediately west of the property hosts Mississippian fauna (J. Monger, pers. comm., 1981) and provides a probable upper age. Ordovician conodonts have been collected by P. Read (pers. comm., 1981) in similar stratigraphy ten kms to the southwest of the property area.

K/Ar determinations on Cr-muscovite yields a mineralization age of 192 ± 7 Ma; which is concordant with the alteration age. It should be noted that these dates are remarkably similar to those obtained from hydrothermal biotite at the nearby porphyry deposits of Schaft Creek (182 ± 6 Ma; Pantaleyev, 1973) and Galore Creek (198 ± 7 Ma; White et al, 1968). Figure 2-2 summarizes the geochronology of mineralization and plutonism for the region.

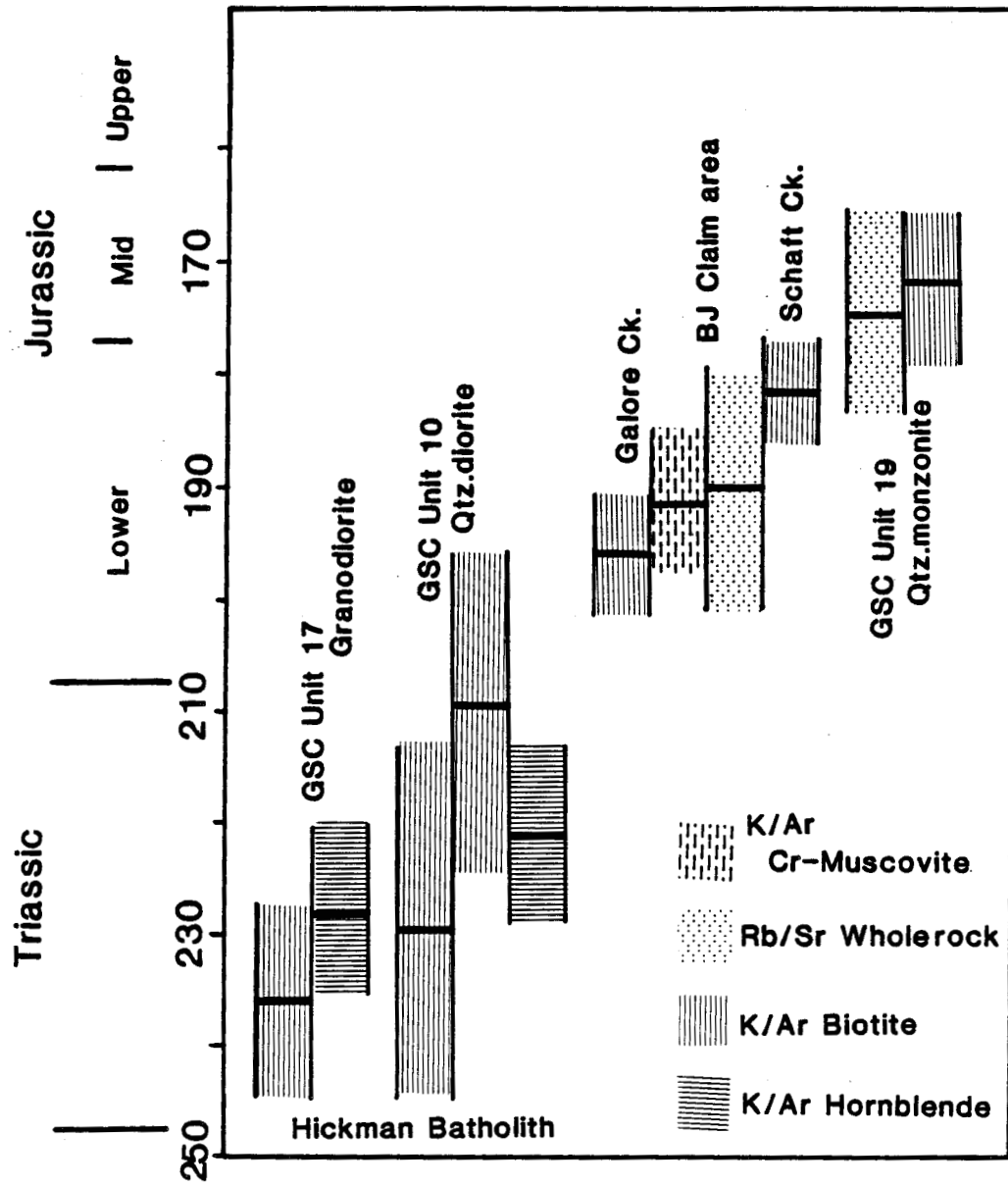


FIGURE 2.2.

Summary of geochronology for mineralization and plutonism in the central Telegraph Creek map sheet area (104G). All determinations by Holbek (in prep.) except where noted in text.

3. LITHOGEOCHEMISTRY

3.1 Methods

Rock samples were collected as chips from two to ten square-metre outcrop areas in order to provide representative specimens. Field duplicates were taken to monitor chemical variance due to sampling. Rocks were ground to -280 mesh, split and lab duplicates were taken. With the exception of gold, all elements were analyzed by X-ray fluorescence of four gm pressed powder pellets. Data reduction was performed on computing facilities at U.B.C. utilizing programs by Vander Hayden (1982) and Berman (1977). All results were calculated on a volatile free basis.

Analytical precision was determined on duplicate pairs using the method of Thompson and Howarth (1976; 1978). Precision varies, both as a function of concentration and the element analyzed. Appendix I is a diagrammatic representation of precision for all elements at 90% and 99% confidence levels. Insufficient duplicate analyses were performed on trace elements with the exception of Cr and V, to make a representative measurement of precision; however, qualitative estimates are shown in Appendix I.

3.2 Major Element Chemistry

Results of major element analyses are presented in Table 3.1. Average analyses for lithological units are also included in Table 3.1. Analyses outside of 1.5 standard deviations were not used in calculation of

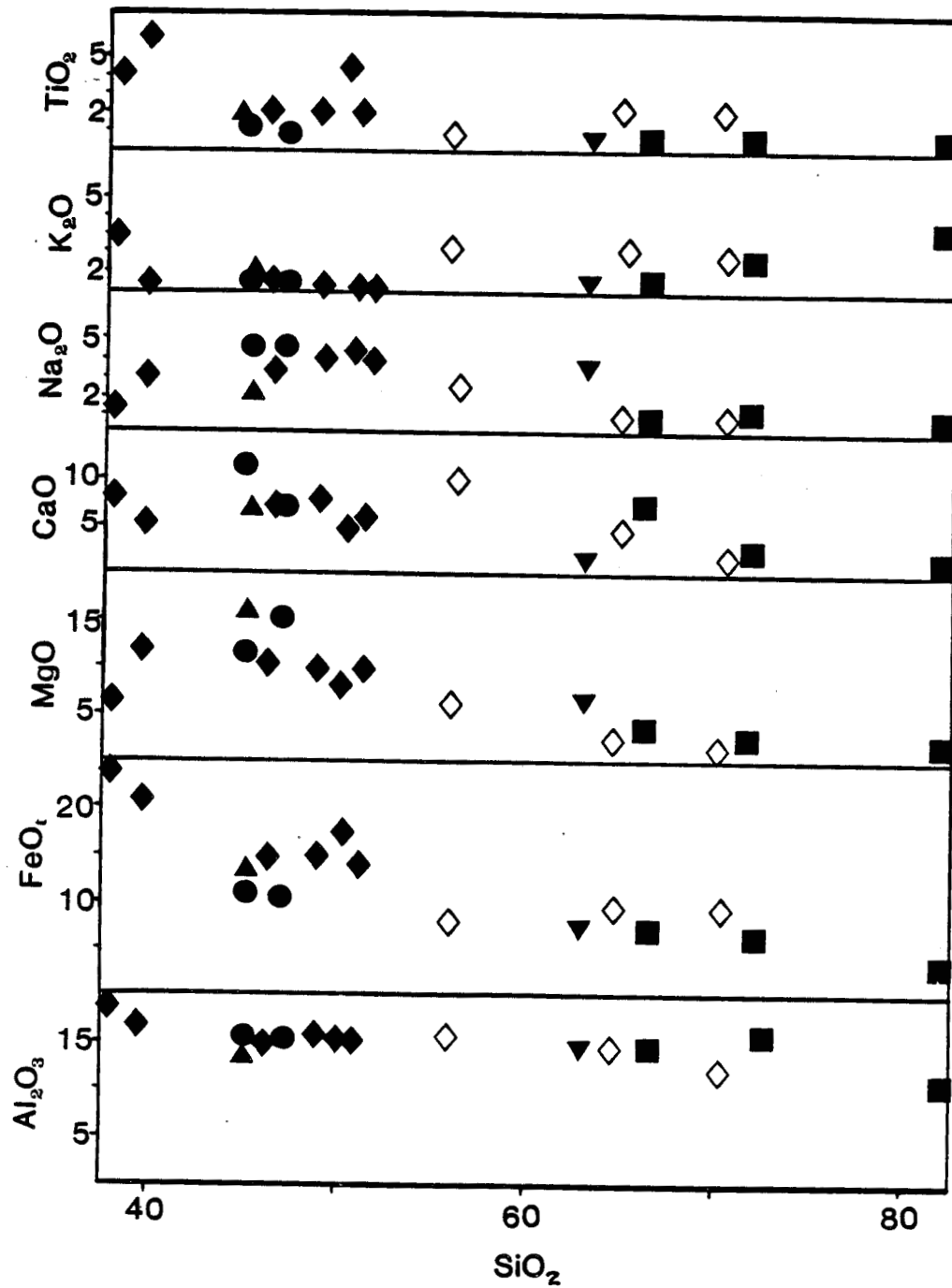
UNIT	CHEM. CLAS.	I. D.	SI	AL	FE	MG	CA	NA	K	TI	MN	P	TOTAL
ARGL		27b1	65.08	17.75	6.01	2.11	1.84	2.40	3.80	1.00	0.17	0.24	100.43
ARGL		27b2	65.20	17.54	5.99	2.25	1.85	2.42	3.73	0.99	0.17	0.23	100.40
PGST	ALKALI BASALT	78b1	45.95	15.79	10.59	11.04	10.53	4.83	0.29	1.11	0.10	0.16	100.41
"	"	78b2	44.62	15.50	10.64	11.74	11.92	4.36	0.40	1.05	0.07	0.15	100.47
QMCS	BASALT	126a	67.19	12.09	4.86	5.55	5.92	1.64	1.72	0.42	0.17	0.08	99.68
CMQS	ANDESITE	126b	68.45	15.60	4.59	3.47	2.78	1.79	2.49	0.59	0.12	0.27	100.18
CHST/GRST		126d	41.59	17.06	19.03	10.54	6.42	1.77	2.17	2.81	0.16	0.40	101.97
GRST	BASALT	126e	50.47	15.68	14.83	8.30	4.24	4.11	0.33	2.36	0.17	0.38	100.90
GRST	HAWIITE	126f	48.20	14.88	14.21	8.69	7.37	4.41	0.44	1.97	0.16	0.37	100.70
PGST?	THOL. BASALT	128a1	55.65	15.41	7.56	5.89	10.19	2.43	2.31	0.58	0.15	0.14	100.33
"	"	128a2	55.43	15.29	7.45	5.60	9.95	2.38	2.32	0.57	0.15	0.15	100.29
GRST	ANDESITE	136b	49.64	17.45	14.21	9.59	1.85	2.83	3.93	1.04	0.17	0.23	100.97
PGST?	PICRITE BASALT	142	48.65	15.42	15.16	9.60	5.12	3.06	1.47	1.87	0.14	0.36	100.87
GRST	K-POOR BASALT	143a	46.92	16.28	16.20	11.02	3.54	3.16	1.31	2.17	0.17	0.31	101.09
"	"	143b	51.03	14.71	12.92	9.76	5.72	3.76	0.32	1.70	0.13	0.34	100.42
QMCS	BASALT	144a2	65.28	15.80	7.94	3.64	3.68	1.44	1.66	0.60	0.15	0.09	100.30
"	ANDESITE	144b1	71.55	15.00	5.13	2.58	2.23	1.22	1.74	0.51	0.12	0.07	100.16
"	"	144b2	71.16	14.91	5.41	2.64	2.23	1.31	1.74	0.51	0.13	0.07	100.15
GRST	PICRITE BASALT	145b1	37.92	17.78	25.68	6.77	7.73	0.81	2.82	4.12	0.11	0.35	101.10
"	"	145b2	37.83	17.97	25.05	6.79	7.23	1.61	2.87	4.12	0.11	0.35	103.95
FVCS	CALC-ALK. AND.	166b	63.64	15.06	7.64	6.85	1.79	3.54	0.58	0.66	0.17	0.11	100.06
GRST	BASALT	173a1	41.96	16.06	16.75	11.14	5.39	2.90	0.10	6.92	0.15	0.67	102.05
"	"	173b1	38.01	15.56	23.21	12.27	3.65	2.88	0.10	6.78	0.17	0.59	103.23
"	"	173a2	38.26	15.51	21.53	12.15	5.47	2.83	0.09	6.09	0.15	0.61	102.71
"	"	173b2	37.92	16.15	22.33	12.30	3.80	2.92	0.11	6.91	0.17	0.54	103.15
GRST	THOL. BASALT	175-1	60.74	11.62	24.18	2.49	1.61	0.61	2.15	0.63	0.60	0.14	104.34
"	"	175-2	60.07	11.73	25.50	2.42	1.42	0.53	2.04	0.62	0.56	0.14	105.05
GRST	THOL. BASALT	176a1	49.89	14.44	13.57	9.22	7.11	3.60	0.54	1.63	0.10	0.40	100.53
"	"	176b1	49.86	13.85	13.32	8.85	8.25	3.76	0.42	1.65	0.09	0.41	100.48
"	"	176a2	47.64	14.99	14.59	9.73	7.35	3.77	0.55	1.62	0.09	0.40	100.75
"	"	176b2	49.34	14.53	13.18	8.93	8.05	3.82	0.44	1.75	0.09	0.40	100.55

TABLE 3.1. Major Element Determinations. a-b subscripts indicate field duplicates; 1-2 subscripts indicate lab duplicates.

UNIT	CHEM. CLAS.	I.D.	SI	AL	FE	MG	CA	NA	K	TI	MN	P	TOTAL
CALT	BASALT	180a1	57.31	16.25	8.41	4.60	9.07	1.48	2.27	0.71	0.17	0.13	100.41
"	"	180a2	57.84	15.91	8.34	4.65	8.97	1.46	2.21	0.66	0.17	0.12	100.34
"	"	180a2	57.82	15.89	8.03	4.52	8.71	2.14	2.22	0.66	0.17	0.11	100.30
ARGL		180b1	81.64	9.74	2.75	1.39	0.57	0.86	2.36	0.27	0.10	0.13	99.82
"		180b2	81.71	9.65	2.83	1.37	0.86	0.44	2.40	0.28	0.10	0.14	99.80
QMCS	ANDESITE	181a	55.04	18.02	12.61	4.62	3.71	2.84	2.61	1.00	0.18	0.33	100.99
QMCS	ANDESITE	181c	49.74	18.60	16.45	4.65	2.53	2.73	5.11	1.28	0.17	0.32	101.61
"	"	181c2	49.78	19.11	16.42	4.54	2.52	2.47	5.10	1.28	0.17	0.32	101.72
CQMS	BASALT	181d	51.58	17.39	13.43	6.15	5.65	2.51	2.75	1.06	0.16	0.31	101.02
CQMS	BASALT	181e	57.99	17.69	10.18	4.68	2.54	1.20	5.02	0.93	0.17	0.25	100.67
QMCS	DACITE	181f	73.33	13.90	2.46	4.03	0.23	0.83	4.82	0.28	0.14	0.03	100.08
CHST	PICRITE BASALT	181g	45.09	13.99	13.37	15.85	7.31	2.21	0.86	0.92	0.12	0.15	99.91
CHST/ALT		184a	55.87	18.58	11.75	3.60	4.17	3.88	1.74	0.98	0.17	0.24	101.00
CHST	PICRITE BASALT	186a1	46.08	14.37	13.88	14.96	5.93	1.58	1.99	0.92	0.15	0.17	100.06
"	"	186a2	46.60	14.06	13.17	15.09	5.72	2.08	1.95	0.88	0.14	0.16	99.88
"	"	186b1	46.55	13.95	12.87	14.94	6.31	2.08	1.97	0.87	0.15	0.14	99.85
"	"	186b2	47.11	14.22	13.13	14.59	6.45	1.29	1.99	0.89	0.15	0.14	99.98
GRST	THOL. ANDESITE	188a1	50.17	14.22	16.99	7.39	3.50	4.47	0.30	3.56	0.25	0.60	101.45
"	"	188b2	50.78	13.36	17.41	7.51	4.04	3.82	0.33	3.69	0.33	0.45	101.73
"	"	188b1	49.77	14.08	17.39	7.74	4.05	3.85	0.33	3.78	0.33	0.48	101.82
"	"	188a2	50.59	14.70	16.59	7.01	3.45	4.52	0.32	3.47	0.25	0.53	101.45
CALT		188c	53.53	16.16	13.31	3.73	7.46	1.25	3.06	2.22	0.27	0.33	101.34
CALT		188d1	69.73	12.36	9.24	1.34	2.23	1.21	1.82	1.40	0.17	0.38	99.90
CALT		188d2	69.78	12.37	9.29	1.30	2.24	1.11	1.83	1.40	0.17	0.37	99.90
CALT		188f	64.32	13.90	9.06	1.93	4.98	0.81	2.50	1.97	0.17	0.31	99.96
PGST	ALKALI BASALT	189a1	43.71	14.90	10.51	12.34	12.17	4.04	0.90	1.36	0.17	0.21	100.32
"	"	189b2	47.30	14.91	10.01	15.10	6.45	3.59	0.97	0.97	0.17	0.11	99.61
"	"	189b1	46.51	15.53	9.90	15.12	6.48	3.86	0.99	0.98	0.17	0.12	99.68
"	"	189a2	45.74	15.00	10.16	11.18	11.48	4.16	0.92	1.30	0.17	0.18	100.31
QMCS	K-RICH BASALT	190a1	68.27	12.61	6.45	3.82	6.45	1.08	0.49	0.36	0.17	0.09	99.82
"	"	190a2	69.09	12.95	6.29	3.71	6.06	0.60	0.50	0.37	0.17	0.10	99.86
"	"	190b2	66.29	13.78	6.99	3.81	7.15	0.61	0.65	0.44	0.18	0.08	99.99
STANDARD		bcr-1	55.64	14.39	12.89	2.80	6.17	3.65	1.57	2.16	0.17	0.31	100.46
"		bcr-1*	54.93	13.72	12.44	3.48	6.97	3.30	1.70	2.26	0.18	0.36	99.99
CHST		average	46.00	14.04	13.32	15.38	6.70	2.01	1.41	0.91	0.13	0.15	100.26
PGST		average	45.55	15.37	10.38	12.42	10.19	4.25	0.65	1.12	0.13	0.14	100.20
FVCS		average	63.64	15.06	7.64	6.85	1.79	3.54	0.58	0.66	0.17	0.11	100.06
GRST		average	49.11	15.30	15.01	9.69	4.52	3.29	0.78	2.28	0.16	0.40	100.54
QMCS/CQMS		average	68.55	14.08	5.34	3.76	3.80	1.26	1.97	0.46	0.15	0.08	99.45

TABLE 3.1 Cont'd.

FIGURE 3.1



Harker variation diagram for major elements. Elements are plotted in weight %.

- Unit 3 PGST
- ▲ " 2 CHST
- ▼ " 4 FVCS
- ◆ " 5 GRST
- ◇ carb. alt. GRST
- Unit A QMCS.

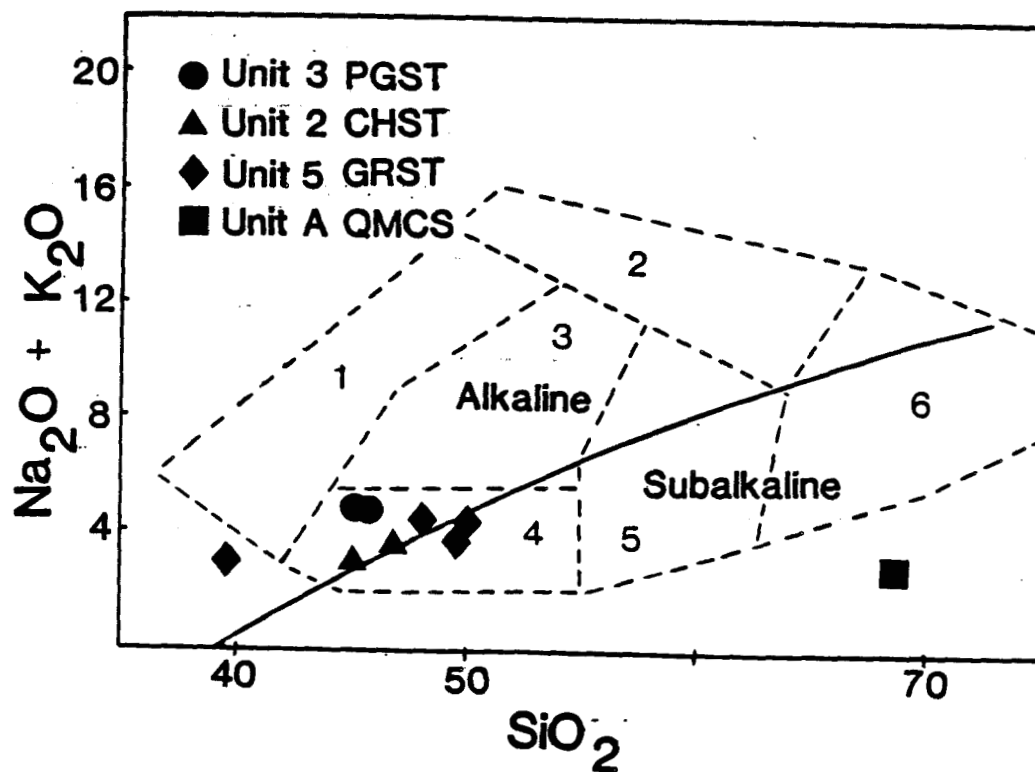


Figure 3.2: Alkalies silica plot with alkaline-subalkaline dividing line from Irvine and Baragar (1971) classification fields after Cox et al (1979): 1-nephelinites and tephrites, 2-phonolites and trachytes, 3-trachybasalts, 4-basalts, 5-andesites, 6-dacites and rhyolites. Unit 3 plots in the alkaline field, units 2 and 5 lie along a tholeiitic trend (see figure 3.3). Average sample for Unit A plots outside of normal classification fields due to metasomatic sodium loss and silica addition.

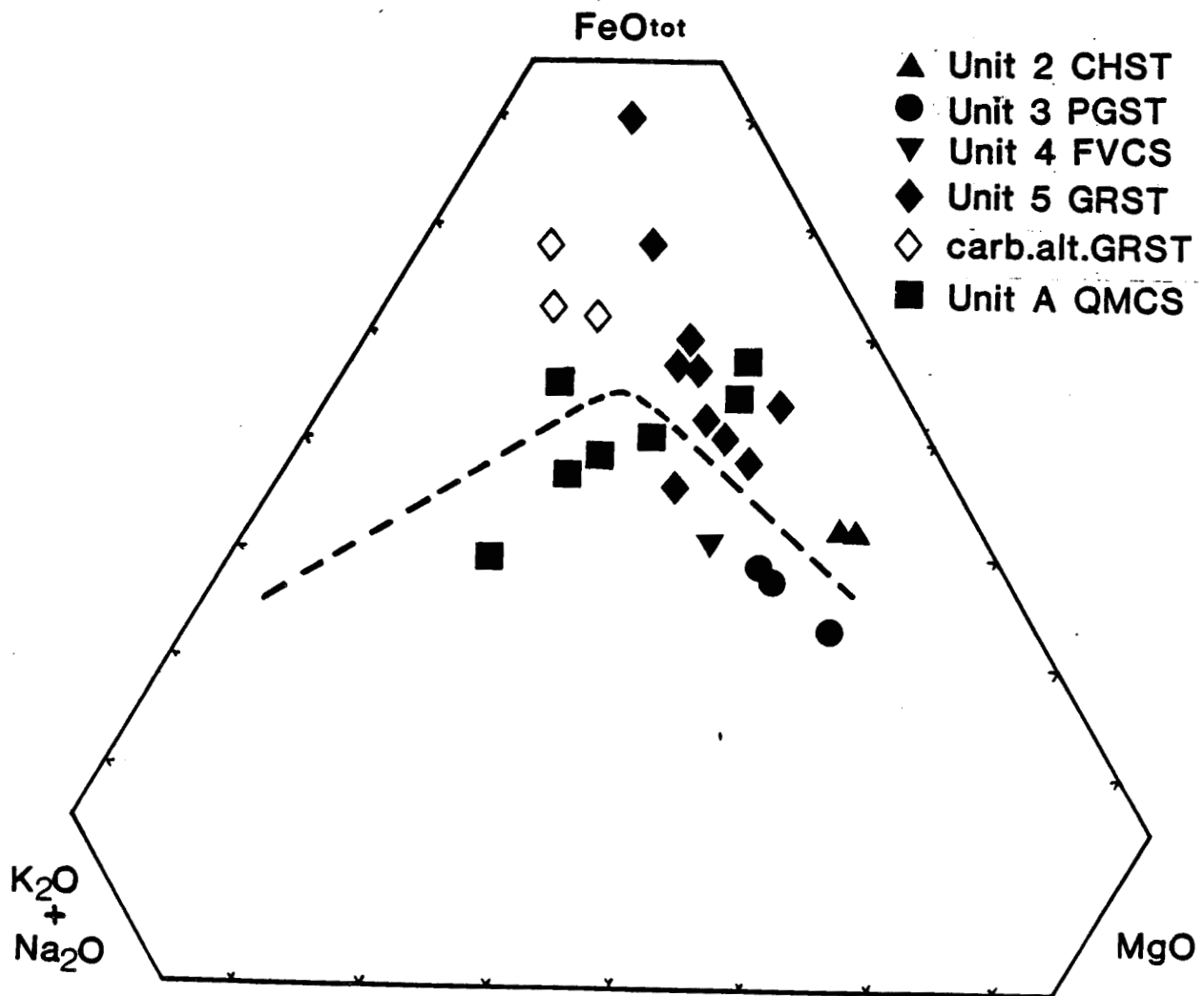


Figure 3.3: AMF diagram plotted from major element chemistry. Tholeiite-calc alkaline dividing line from Irving and Baragar (1971). Unit 5 plots in the tholeiite field. Unit A displays a weak differentiation trend.

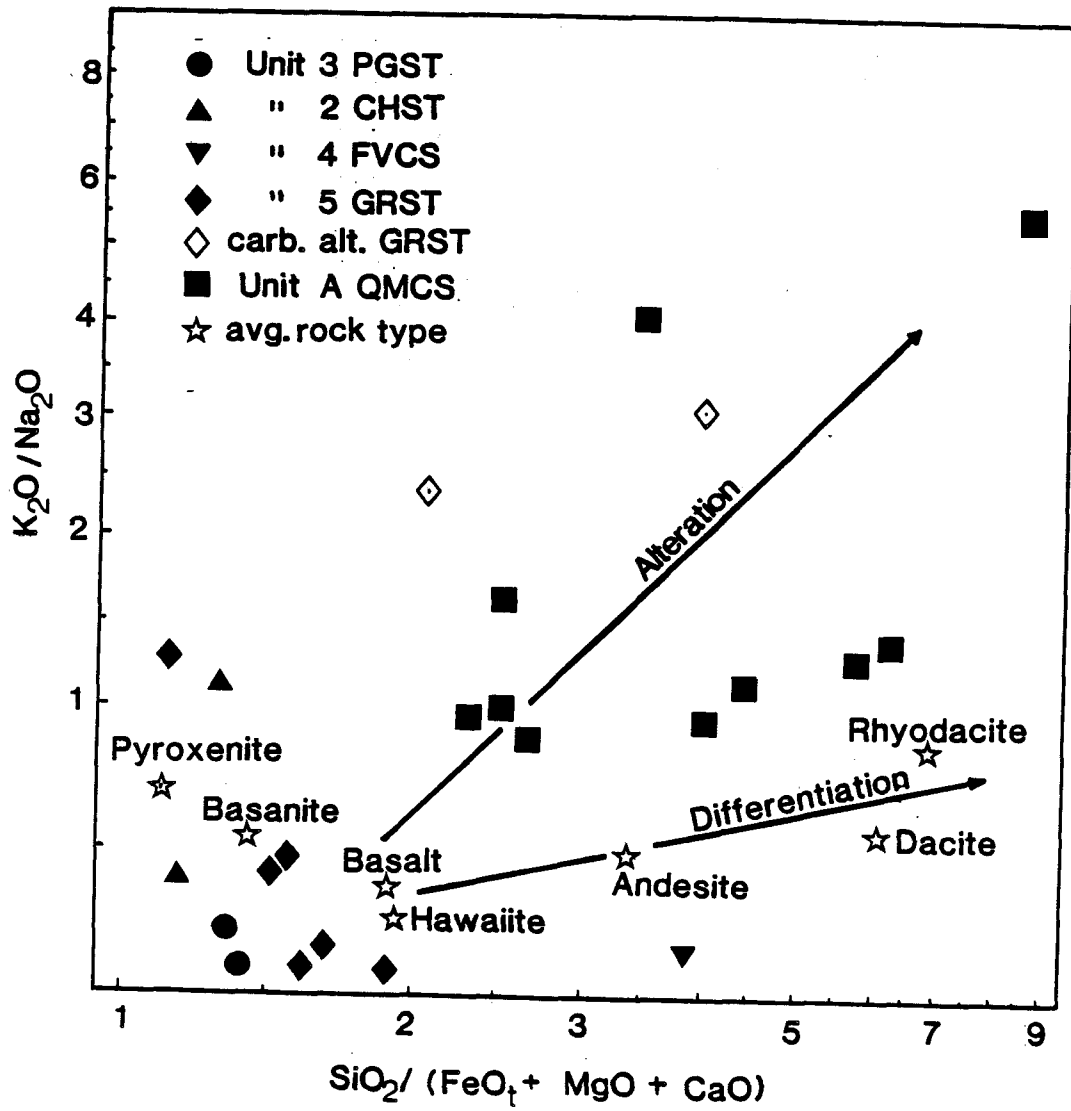


Figure 3.4: Plot of potassium/sodium vs. silica/ferromagnesian elements with magmatic differentiation trend based on average rock compositions (Le Maitre, 1976). Wide scatter and high potassium/sodium ratio of unit A samples is likely a function of both differentiation and alteration.

averages. A correlation matrix for major and trace elements can be found in Appendix II.

Figure 3.1 is a Harker variation diagram showing elemental concentration as a function of silica content. Lithological subdivisions are supported by chemistry with Si, Fe, Mg and Ti showing the greatest variations. All elements display a negative correlation with Si except for Al which remains unchanged. Depletion of Na with increasing silica is anomalous with respect to rock-forming processes.

Chemical classification and nomenclature of volcanic rocks according to the system of Irvine and Baragar (1971) are shown in Figures 3.2, 3.3 and Table 3.1. Figure 3.2 is an alkalis-silica plot and shows the alkalic character of Unit 3. Units 2 and 5 are not effectively classified by Figure 3.2, but plot in the tholeiite field of Figure 3.3. The average composition of the Unit A samples plots outside of the standard classification fields of Figure 3.2 due to considerable sodium depletion. On the AFM diagram (Figure 3.3), Unit A displays a partial magmatic differentiation trend.

3.3 Trace Element Chemistry

Results of trace element analyses are shown in Table 3.2. Primary use of trace element data is to further aid chemical classification and to provide constraints on magmatic affinities and plate tectonic setting. Trace elements have an advantage over major elements in that they are

less mobile during syngenetic or subsequent alteration.

The Zr-Ti-Y ternary discrimination diagram (Figure 3.5) after Pearce and Cann (1975) indicates a within plate origin for BJ basalts. Since a continental origin is unlikely for an accretionary terrain, an ocean island setting is implied. This implication is also reached via a Ti-Cr plot (Garcia 1978) and Y/Nb ratios (Pearce and Cann 1975). The high Ni and Cr content of Unit 3 and Fe, Ti content Unit 5 is also characteristic of primitive magmas erupted as ocean islands (Irvine and Baragar 1971). The discrepancy between Unit A and the other Units in Figure 3.5 is due to either Ti loss or that those samples were not basalts. The association of alkalic and tholeiitic basalts and major element chemistry are very compatible with an ocean island setting.

Much of the above is only significant if the trace elements used have not changed their ratios since magmatic crystallization. Ti and Zr have been shown to be immobile, even during hydrothermal alteration (Finlow-Bates and Stumpf 1981). Figure 3. shows Al, Ti and Zr ratios plotted against MgO, Zr and Ti ratios with Al normalize the constant sum effect during gain or loss of silica. The constant Al/Zr ratio for the various lithologies, over a range of MgO values, indicates lack of Zr mobility. Al/Ti ratios display a sympathetic trend with MgO except for a marked diversion of Unit A and altered samples. The scatter within Unit A and the slight rise of Al/Ti of the altered chlorite schists suggests limited Ti mobility. The unique grouping of Unit A Zr/Ti

SAMPLE I.D.	ROCK TYPE	CHEM. CLASS.	Nb	Zr	Y	Sr	ppm		Cr	V	Ce	Nd	Au (ppb)
							Rb	Ni					
27a ₁	ARGL	-					5	2	104	74	40	1	
27a ₂	ARGL	-					20	22	93	69	31	1	
78b ₁	PGST	Alkali basalt	17	74	30	269	1	210	329	173	29	<1	8
78b ₂	PGST	Alkali basalt						205	316	170	57	12	2
126 a	QMCS	Basalt	15	121	22	173	31	45	110	71	65	9	
126b	QMCS	Andesite	20	146	43	238	40	62	68	95	77	12	1
126d	CHST	Basalt	20	145	32	162	29	32	65	381	53	19	1
126e	CALT/GRST	Basalt	20	138	38	102	4	20	78	358	36	9	12
126f	GRST	Hawaiite	20	154	35	415	8	23	78	350	36	10	1
128a ₁	?	K-rich basalt	18	165	36	310	38		106	126	109	21	
128a ₂	?	K-rich basalt						39	111	143			
136b	CALT	Andesite	20	122	32	81	78	3	13	207	35	7	
142	GRST	Basalt	18	169	42	445	23		60	329	26	34	
143a	GRST	Picrite basalt	19	158	40	260	12		59	345	16	12	7
143b	GRST	K-poor basalt						23	26	383	21	19	2
144a ₂	QMCS	Basalt	18	154	36	149	32	9	21	94	56	8	2
144b ₂	QMCS	Andesite	19	156	33	157	31	6	68	83	49	12	1
145b ₁	GRST	-						20	12	485	65	5	
145b ₂	GRST	-						24	22	523	69	4	
166B	FVCS	Dacite						110	74	83	27	6	
173a ₁	GRST	K-poor basalt	21	198	27	252	<1	4	15	412	30	48	34
175-1	CALT/GRST							33	86	132	240	31	
176a ₁	GRST	Picrite basalt						11	47	370	26	25	1
180a	?	Basalt							118	126	62	11	2
181a	QMCS	Andesite	20	99	26	199	57	3	29	161	56	10	1
181c	QMCS	Andesite	18	114	39	207	112	5	5	235	36	10	2
181d	CHST	Basalt	17	99	26	199	57	5	29	210	36	7	4
181e	CHST	Basalt	14	110	18	270	104	11	58	194	22	<1	6
181f	QMCS	Dacite	24	271	<1	9	96	11	53	71	174	48	1
181g	CHST	Picrite basalt	18	64	20	566	13	58	21	449	15	5	2
184	CALT/CHST	Basalt	17	110	24	234	36	4	39	154	44	14	
186a ₁	CHST	Picrite basalt						63	58	452	24	18	1
188a ₁	GRST	Basalt	22	191	43	192	<1		5	427	49	15	1
188a ₂	GRST	Andesite	23	196	47	199	3		14	470	19	12	1
188c	CALT	-						5	61	378	919	15	
188d	CALT	-						4	89	134	215	<1	
188f	CALT	-	15	106	24	1031	30		87	182	106	28	
189a ₁	PGST	Alkali basalt	16	77	24	208	16	114	256	244	18	<1	1
189b ₁	PGST	Alkali basalt						120	198	222	<1	14	1
189b ₂	PGST	Alkali basalt	17	76	25	203	15	120	182	234	5	<1	1
190a ₁	QMCS	K-rich basalt	18	130	31	117	7				57	13	1
190a ₂	QMCS	K-rich basalt	18	130	33	118	5				14	26	3
190b ₂	QMCS	K-rich basalt							78	69	71	7	2
RC4	MINZ	-											

TABLE 3.3: TRACE ELEMENT DETERMINATIONS

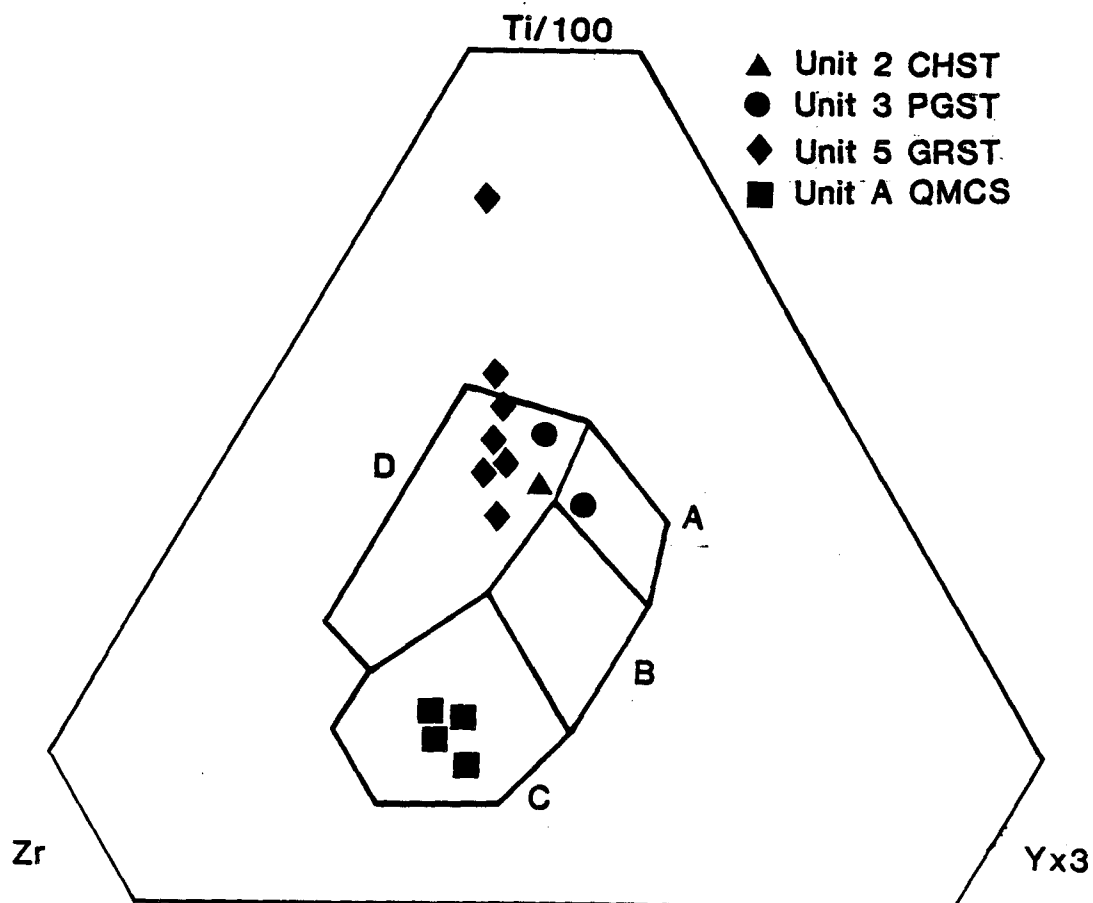


Figure 3. : Ternary discrimination diagram after Pearce and Cann (1975). Fields differentiate between plate tectonic settings for basalts: Within plate - ocean island or continental* basalts plot in field D; Ocean floor basalts in field B; low potassium tholeiites in fields A and B; calc-alkali basalts in fields C and B.

BJ basalts plot as within plate basalts. Assuming that all BJ volcanics have a common tectonic origin, unit A plots in field C either because samples have undergone Ti loss or that they were not originally basalts.

*Recent work has demonstrated that this diagram is not suitable for continental basalts (Holms, 1982).

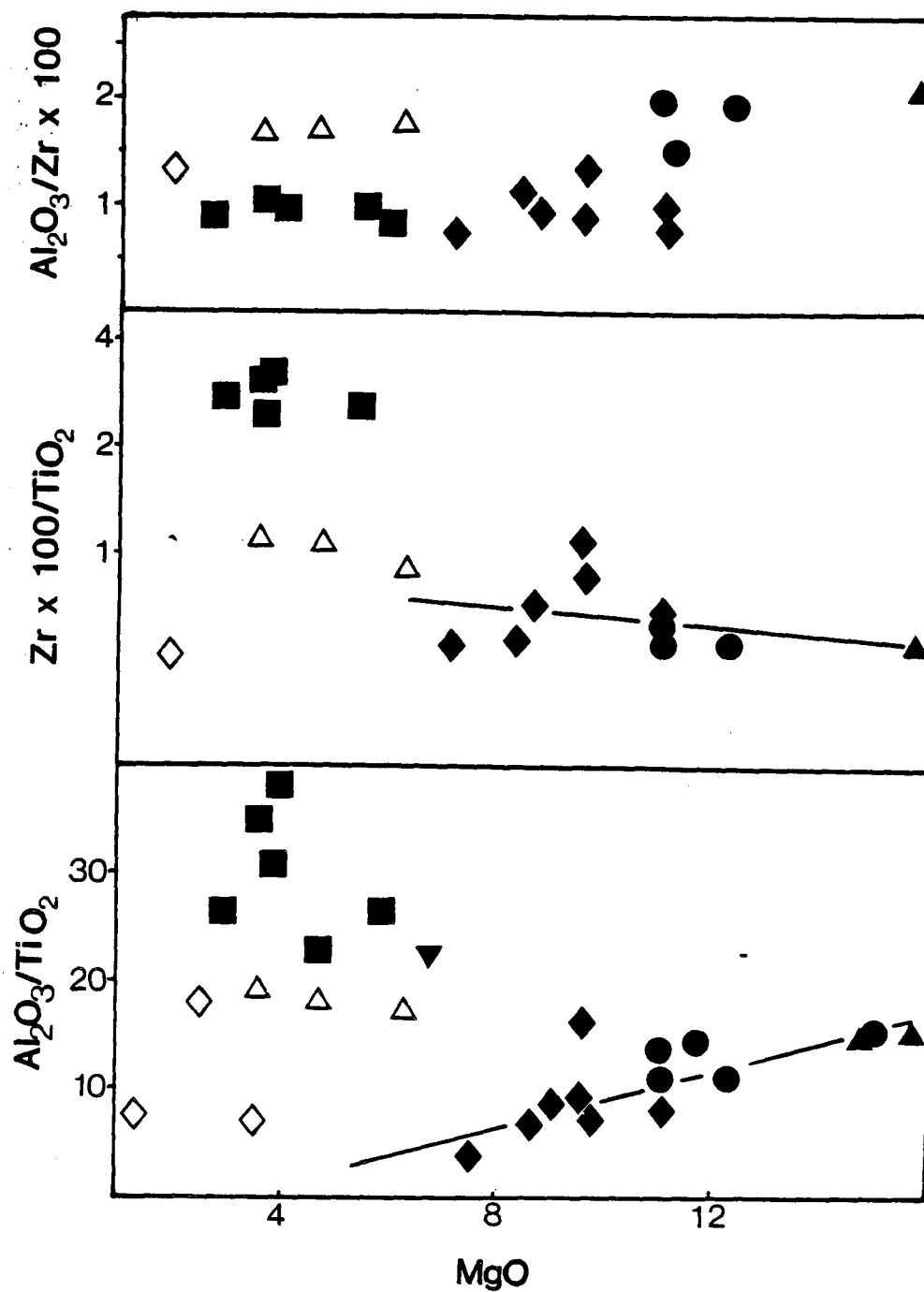


Figure 3. : Al, Ti and Zr ratios plotted against MgO. Al ratios provide a normalization factor in the event of loss or addition of silica. Hollow symbols indicate altered rocks of known parentage. Rocks show consistent Al/Zr ratios over a range of MgO, attesting to the relative immobility of Zr. Al/Ti ratios display a sympathetic trend with MgO except for a marked diversion of Units 4 and A. The slight rise in the Al/Ti ratios of altered chlorite schists and the scatter in unit A suggests some Ti mobility. The marked increase in Zr/Ti ratios of unit A indicates that its deviation from other units was controlled more by primary magmatic processes than by alteration.

ratios indicates a separate rock type for these samples. This Zr/Ti ratio of about 3 is typical of dacitic compositions (Floyd and Winchester 1978). It should be noted however that the altered samples of Unit 2 are visually both macro and microscopically indistinguishable from Unit A samples. Therefore, Zr and T analyses can provide useful guides to the parentage of altered rocks.

Y analyses are extremely well behaved and do not appear to be affected by alteration.

4. ALTERATION AND MINERALIZATION

4.1 Description of Mineralization

Rocks containing elevated precious metal values occur in several distinct settings. Occurrences can be divided into silica or carbonate dominated systems. Further subdivisions can be made on the basis of morphology, textures and mineral assemblage. In the order of paragenetic sequence the subdivisions are: 1) metamorphogenic quartz-pyrite veins; 2) disseminated sulphides in carbonate alteration zones; 3) carbonate-sulphide veins; 4) quartz-chalcopyrite veins; and 5) quartz breccia veins. Superimposition and gradations between groups often make strict classification difficult. Details of the various groups are given below.

1) Metamorphogenic quartz-pyrite veins.

These veins are ubiquitous to the property and surrounding area. Dimensions are highly variable, but irregular, sub-continuous, lenticular morphology is standard. Silica-potassic alteration peripheral to veins is common. Most veins are concordant, either lying along foliation planes or concentrated in zones of dilation such as fold noses. Veins are synchronous with the first phase of deformation and have been deformed by subsequent phases.

Veins consist of coarse grained, milky quartz with coarse euhedral pyrite. Chalcopyrite is associated, but other sulphides are scarce. Gold values are generally low, ranging from mildly anomalous to potentially ore grade in rare sulphide rich pods.

The only significant showing in this group is the telluride vein in the central area of the Jay chain. The vein is conformable, exposed over a distance of 180 m and hosts a mineral assemblage including: gold, hessite, tetradymite, tellurobismuthite, galena, tetrahedrite, sphalerite, chalcopyrite and pyrite. The gold assay was disappointing, yielding only 0.014 oz/t. Vein margins are indistinct showing gradually increasing silicification of wall rocks. Faint outlines of ghost fragments, which still maintain structural conformity with wall rocks, indicate passive emplacement.

2) Quartz breccia veins.

These veins are easily distinguished by their cross-cutting relationships and breccia textures. Breccia fragments are angular to subrounded chunks of wall rock in varying stages of silification; suggesting forceful emplacement of veins. Mineralization consists of pyrite, galena, sphalerite and gold hosted by fine grained, grey, glassy quartz and minor barite. Grades of up to 0.412 oz/t Au, with an Ag:Au ratio of 8:1 have been obtained within this type of mineralization.

3) Quartz-chalcopyrite veins in carbonate alteration zones.

These veins are likely synchronous to the quartz breccia veins. Veins are commonly dark to light grey and glassy but can be milky and occur exclusively within iron-carbonate alteration zones in greenstones. Coarse amoeboid chalcopyrite with lesser tetrahedrite is characteristic. In general, veins are narrow and sinuous, and do not constitute an appreciable tonnage. The best showing of this

type is on the Wish claim.

4) Carbonate-sulphide veins.

Steeply dipping and fracture controlled, these veins have sharp contacts with their wall rocks which are usually altered to fuchsite, sericite, carbonate, quartz schists. Breccia textures, with both wall rock and vein fragments indicate multiple stages of formation. Sulphides range from massive to granular pyrite and arsenopyrite through to scattered coarse blebs of sphalerite, chalcopyrite and galena in a matrix of mangosiderite. Frierberigite commonly occurs between carbonate bands or breccia fragments. Gold distribution is erratic with the same location giving samples of 2.0 oz/t and 0.2 oz/t. Carbonate sulphide breccia veins are located on the Snout, Grey and Jay claims.

5) Carbonate alteration zones.

Restricted to massive chlorite schists and greenstones, these conspicuous zones of oxidation and carbonization are common over much of the property area.

Zones may be related to either carbonate-sulphide breccia veins or small stock works of quartz-chalcopyrite veins. Sulphides are typically medium grained disseminated pyrite and lesser arsenopyrite. Grades in these zones range from 0.03 oz/t Au to 0.09 oz/t Au. Gold occurs as micro grains within the pyrite and along hair-line silica fracture fillings. Although sub-economic, these zones occur in sufficient quantity and size to account for widespread anomalous gold geochemistry.

4.2 Sulphide Mineralogy and Paragenesis

4.2.1 Mineralogy

Pyrite

Pyrite is the most abundant sulphide with rock volume ranging to 50% and an average of 10%. The pyrite occurs as euhedral to anhedral disseminated grains and as angular crystal aggregates. The size of the pyrite varies between 2 mm and .001 mm wide. Pyrite is disseminated throughout the quartz-carbonate host rock as well as occurring in micro- to macro-quartz veins. Occasionally, the pyrite shows rounding due to shearing along fault planes. Cleavages are sometimes visible in the pyrite along with other textures such as syneresis cracks and penetration twins. Most of the pyrite contains encapsulated gangue. The pyrite also contains chalcopyrite, tetrahedrite, sphalerite, pyrrhotite and hematite. Most of the minerals are trapped via the crystallization of pyrite, but in the case of pyrrhotite, it occurs as a replacement texture. In several samples, pyrite shows extreme replacement by hematite; one case in particular, the hematite replaces pyrite preferentially along cleavage planes. Many minerals form around the pyrite and occur as crack fillings. Examples of these are tetrahedrite, chalcopyrite, sphalerite, galena, and hessite. The pyrite is also intergrown with arsenopyrite and in one polished section it is observed completely contained within a rhombic shaped arsenopyrite crystal aggregate.

Tetrahedrite

The tetrahedrite occurs as irregular convex shaped blebs. There seems to be varying amounts of arsenic as indicated by variations in the intensity in the characteristic green tint. Tetrahedrite is quite abundant in the rock suite with values ranging to 15% and size grading to 5 mm. The tetrahedrite is commonly intergrown with chalcopyrite, as well as with hessite and galena on rare occasions. Tetrahedrite is associated with all minerals identified in the suite and is commonly found enclosing pyrite, sphalerite and arsenopyrite. It is also found as trapped grains within the pyrite and arsenopyrite and within quartz veins with pyrite, sphalerite, and gold. Oxidation of the tetrahedrite is visible where a tiny quartz vein crosscuts a tetrahedrite grain creating selvages of cuprite. It is possible that some chalcopyrite present in the tetrahedrite is the result of exsolution and not just simply an intergrowth. Friebergite (Ag = 15-20%) occurs as coarse irregular grains associated with chalcopyrite and pyrite in mango-siderite veins and breccias.

Chalcopyrite

This mineral occurs in all the polished sections studied with values ranging to 5%. The chalcopyrite occurs as isolated irregular convex shaped blebs with sizes grading to 2 mm and as intergrowths with the tetrahedrite. The chalcopyrite also quite commonly occurs as exsolution lamellae and blebs within the sphalerite. The orientation of

the chalcopyrite is dependant upon the cleavage directions of sphalerite. There is some possibility that a small proportion of the chalcopyrite is the product of exsolving from the tetrahedrite. Chalcopyrite is commonly observed filling cracks in and around the pyrite and the arsenopyrite as well as being contained within the pyrite and arsenopyrite crystal aggregates and grains. Definite replacement texture is noted where chalcopyrite altered to cuprite via oxidation. This occurs as a reaction rim around the chalcopyrite.

Sphalerite

The mode of sphalerite can reach as high as 15%, as in P.S. Rat-A, and is quite common to the system. The sphalerite crystals are bimodal in the size distribution. The shape of the larger sphalerite grains are rhombohedrons with size ranging to 2 mm.

The smaller sphalerite grains are around .04 mm and occur as lathes to semi-circular crystals. Sphalerite occurs with most other minerals and is intergrown with chalcopyrite.

In most cases, the sphalerite exhibits exsolution blebs and lamellae of chalcopyrite with minor amounts of eskebornite. The exsolution blebs are more concentrated near the edge of the sphalerite. In one sample, the sphalerite within the quartz veins is nearly devoid of any chalcopyrite and it has an orange-yellow internal reflection suggesting a high to intermediate iron content.

Arsenopyrite

Values to 30% and usually occurring as subhedral to anhedral grains which exhibit the characteristic rhomb shape along with rectangular and wedge shapes. The arsenopyrite is observed containing up to 45% encapsulated gangue within crystal aggregates. The crystals also show moderate segmentation with variable fracturing. The mineral occurs as isolated grains, as angular crystal aggregates, intergrown with pyrite aggregates, and in microquartz veins (approximately 2 mm). Like pyrite, arsenopyrite also contains many entrapped minerals, such as tetrahedrite, chalcopyrite, sphalerite, and hematite. On rare occasions, blebs of chalcopyrite can be observed within the arsenopyrite suggesting that the chalcopyrite might have exsolved from the arsenopyrite. Minerals, such as tetrahedrite and chalcopyrite, form within fracture and/or segments of arsenopyrite, while hematite, on the other hand, commonly shows moderate to strong replacement of the arsenopyrite.

Hematite

From samples observed, the hematite can reach a concentration of 5%, and occurs as very small (.04 mm) needle shaped crystal aggregates and as replacement lathes within pyrite and arsenopyrite. In one polished section studied, the hematite selectively replaced pyrite along the cleavages and following dissolution of the pyrite, a grid pattern of hematite was left.

The hematite is also seen as pseudomorphs after wedge-shaped arsenopyrite. A great proportion of hematite is found exhibiting

the characteristic worm-tube structure. This structure forms around grains of chalcopyrite and tetrahedrite as an oxidation rind.

Cuprite

Occurs as a reaction rim forming around chalcopyrite and tetrahedrite blebs and as selvages of a micro-quartz vein which cuts through irregular blebs of tetrahedrite. The cuprite is in contact with the chalcopyrite, tetrahedrite, hematite, and pyrite. The thickness of the rim is approximately .002 mm.

Galena

Somewhat restricted in occurrence, galena occurs as irregular convex shaped blebs growing around pyrite and sphalerite, and intergrown with tetrahedrite. All locations containing galena also host gold (however, the reverse relationship is not true).

Tellurides

Silver and bismuth tellurides occur as thin bands and irregular blebs with pyrite, galena and gold. Based on relative elemental proportions in discreet phases, as determined by SEM/EDS, the following minerals are likely present: hessite, tetradymite and tellurobismuthite. This assemblage has only been found in a single location.

Eskebornite

A tentative identification, this mineral occurs intergrown with chalcopyrite as an exsolution lamellae of sphalerite. The long thin bleb is approximately .01 mm long. Eskebornite also occurs as much smaller blebs contained within the sphalerite grain.

Pyrrhotite

Occurs as exsolution feature in pyrite grains. The size of the blebs are in the order of .01 mm. Pyrrhotite is extremely rare and only 6 blebs have been located in one of the samples.

Gold and Electrum

Quite rare within the rock suite studied, the presence of gold shows no correlation with assay results. Gold was observed in samples with assays ≤ 0.015 oz/t and only a tiny grain of electrum was found in a sample assaying > 2.00 oz/t Au suggesting an inhomogeneous and erratic distribution.

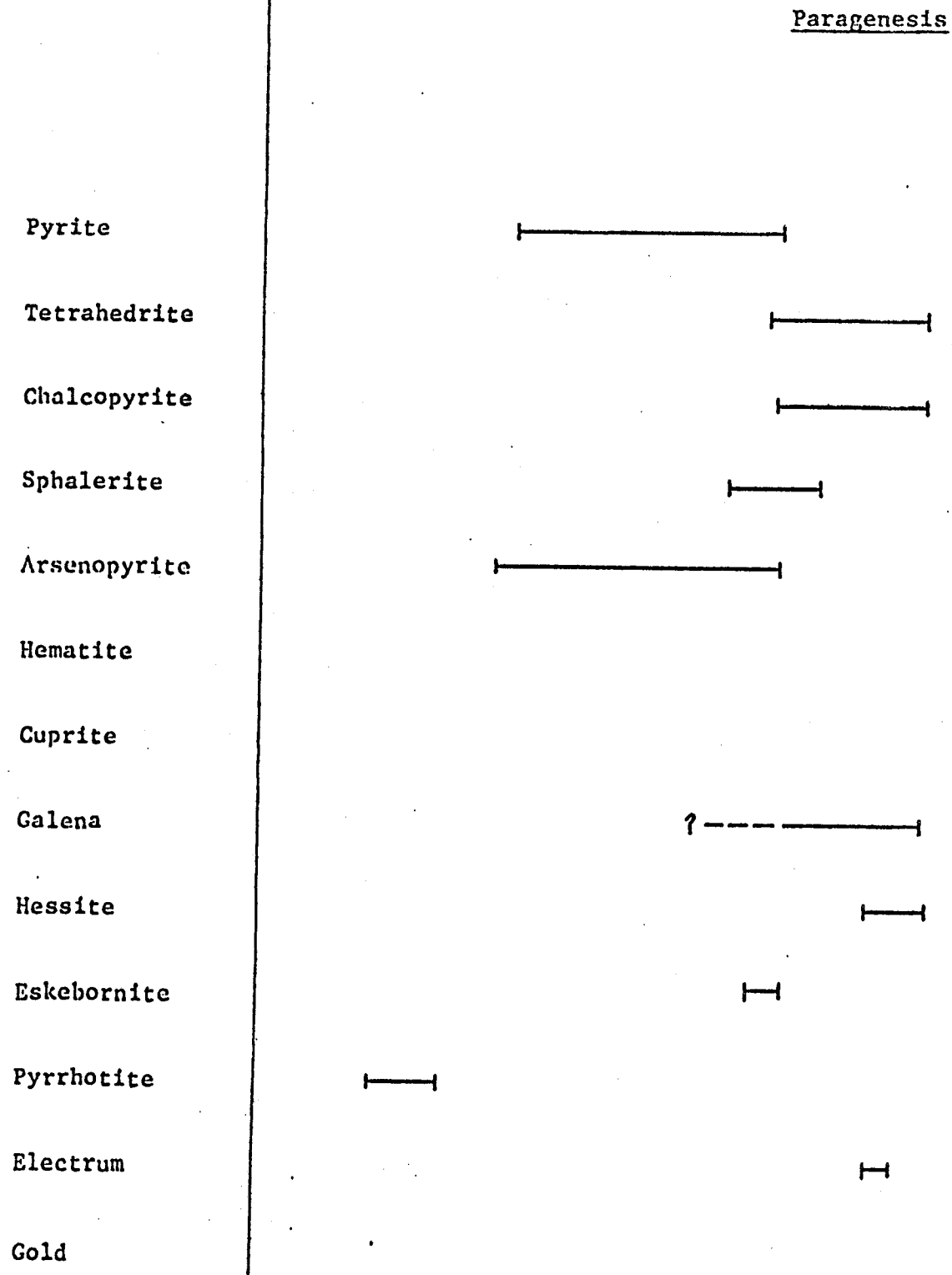
Gold/electrum varies in shape from rounded to highly anhedral and is associated with tellurides and sphalerite, and occurs free in both quartz and siderite. In all observations gold minerals were extremely fine grained (≤ 0.004 mm).

4.2.2 Geothermometry and Paragenesis

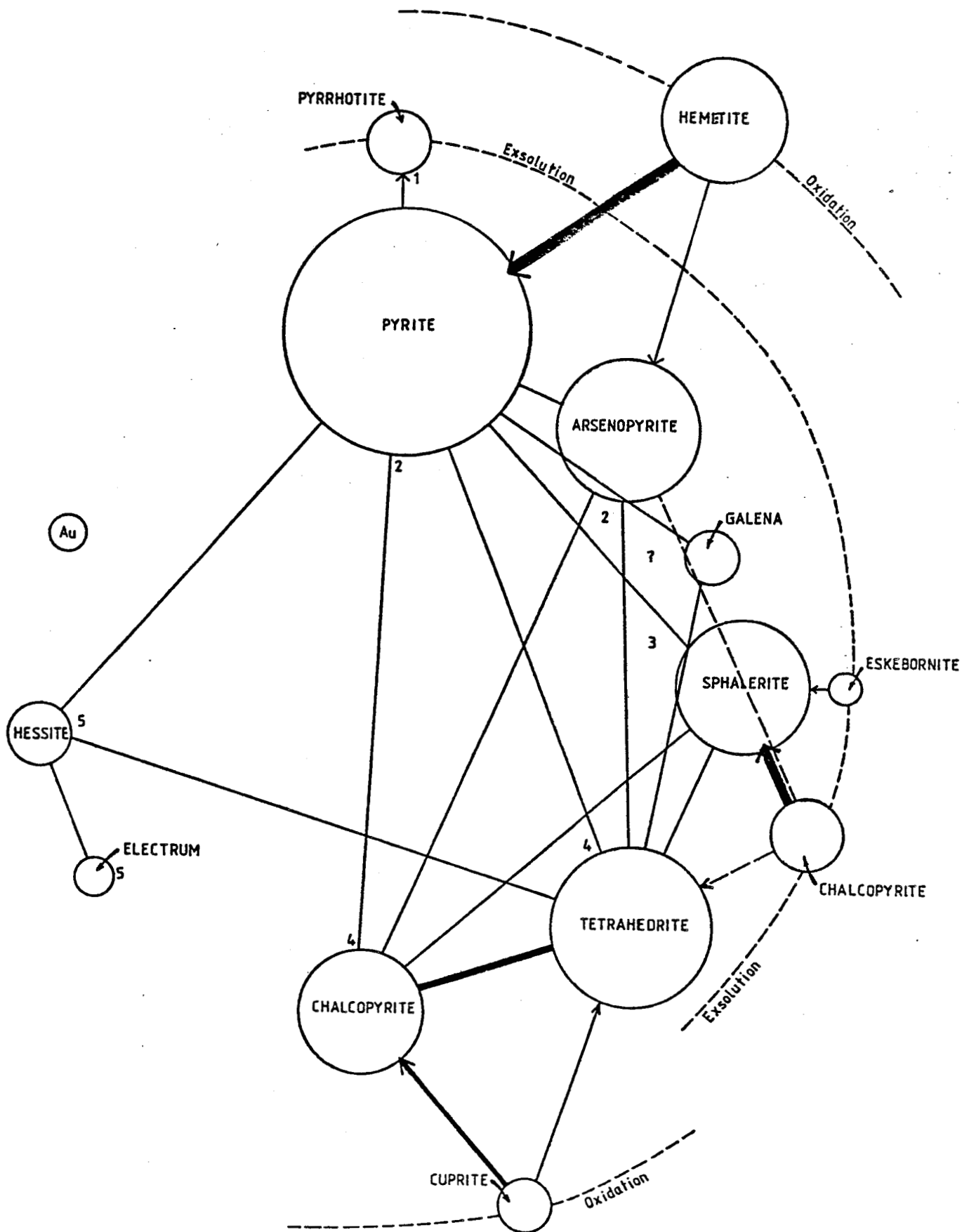
The maximum temperature of formation, given by the pyrite - arsenopyrite assemblage, is $491 \pm 12^{\circ}$ (Clark, 1960). However, the overall assemblage, particularly the sulphosalts, suggest lower crystallization temperatures. Silicate assemblages in vein related alteration indicate temperatures above 150° and up to 490°C .

The mineral to first appear in the crystallizing melt was pyrrhotite. This crystallized incongruently to finally form

pyrite. The arsenopyrite occurred at roughly the same time with both sulphides entrapping newly crystallized quartz carbonate gangue within their subhedral crystal aggregates. The next stage saw the appearance of sphalerite, followed closely by chalcopyrite and tetrahedrite. This was followed in the paragenesis by the exsolving of chalcopyrite and eskebornite from the sphalerite, and chalcopyrite exsolving from the tetrahedrite. A small amount of these minerals were included in the pyrite and arsenopyrite crystal aggregates. By this time, the pyrite and arsenopyrite had almost finished their preveining crystallization. Sometime between the initial crystallization of the pyrrhotite and the final crystallization of the preveining pyrite et al, the mineral galena crystallized. As temperatures dropped to around 200^o, gold, electrum, and hessite crystallized along with low temperature tetrahedrite and vein related pyrite, arsenopyrite, sphalerite and galena. The hessite and electrum crystallized out of the sulphide melt together, leaving behind tetrahedrite which crystallized slightly later; while the gold crystallized as irregular to subrounded blebs within quartz-pyrite-tetrahedrite microveins during the last stages of crystallization. Later, the fully crystallized assemblage was exposed to an oxidizing environment which caused the replacement of pyrite and arsenopyrite by hematite, along with dissolution of both sulphides. Chalcopyrite and tetrahedrite were both oxidized to cuprite.



Paragenesis



4.3 Petrology of Alteration.

Two types of alteration are evident: a silica-potassic alteration and a carbonate-oxide alteration. Type of alteration is controlled by structure and lithology. Carbonate-oxide alteration is most conspicuous in greenstones and chlorite schists (Fe-rich rocks) whereas silica-potassic alteration predominates in the other units. Alteration types are superimposed where carbonate-sulphide veins cut earlier silica-potassic alteration.

4.3.1 Silica-Potassic Alteration.

Occurs as selvages and larger zones peripheral to quartz-pyrite veins and as large zones covering areas up to 12 square km. Contacts with other units are always gradational, except for some greenstone contacts which are relatively sharp. Mineralogy is characteristically extremely fine grained, deformed and made up of variable proportions of quartz, carbonate, muscovite and accessories. Chlorite and fluorite are common in minor amounts. Carbonate compositions, calcite, dolomite and siderite, appear to be controlled by bulk rock chemistry. Very tiny grains of apatite and galena are evenly disseminated throughout. Fuchsite is abundant at some localities. Rutile is common but generally shows disequilibrium textures. Garnet has tentatively been identified at two locations and barite can occur, but is not common. Porphyroblastic monazite is frequently encountered.

The origin of this unit is not straightforward. Major and trace element chemistry indicate varying degrees of alteration within different parent rocks. Field and chemical evidence demonstrate that almost all units can form this alteration product but the majority likely formed from felsic tuffs. Presence of graphite within alteration zones, ubiquitous carbonate and muscovite, and sodium depletion suggest alteration by acid fluids with $\text{CO}_2 \gg \text{H}_2\text{O}$, $\text{K}^+ > \text{Na}^+$ and high fluid:rock ratio. Alteration occurred early in the deformational sequence of the area.

4.3.2 Carbonate Oxide Alteration.

This late stage alteration is strongly fracture controlled and affects all units but is only conspicuous within chlorite schists and greenstones. Mineralogical changes of altered rocks consist of the breakdown of silicates to form carbonates, quartz and sulphides, and oxidation of ilmenite and magnetite to rutile and hematite. Carbonates are dolomite and siderite with lesser quantities of calcite.

The large carbonate zone in the northwest portion of the BJ claim is somewhat anomalous. Over 800m long and 100m wide, it consists of a central core of pure, coarsely banded and botryoidal carbonate ($(\text{Ca}.7, \text{Fe}.2, \text{Mg}.1) \text{CO}_3$) with edges of coarse carbonate breccias. Breccia fragments are large silicified and pyritized blocks of greenstone.

An exotic assemblage of xenotime (Y (REE) PO_4), monazite, apatite, hematite, zircon and barite in a matrix of quartz,

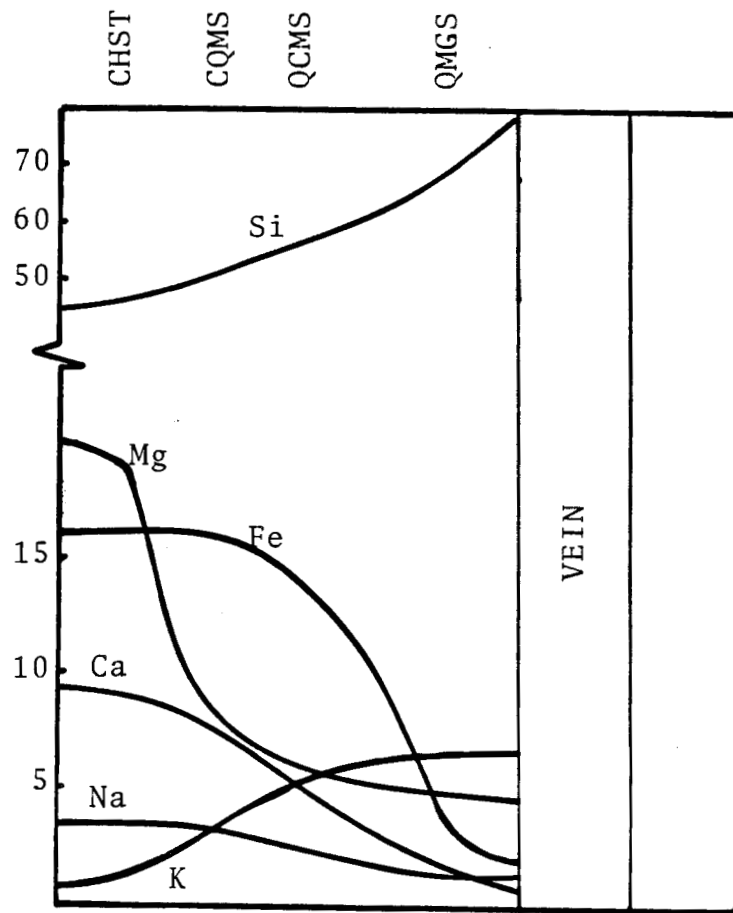


Figure 4.3. Major element variation across silica-potassic alteration peripheral to a quartz-pyrite vein in chlorite schists. Relative proportions of minerals given by deviated rock name: Q = quartz; M = muscovite; C = chlorite; G = carbonate; S = schist.

siderite, and muscovite has been noted in two localities. Xenotime contains up to 40% heavy rare earths, particularly Dy, Er and Yb while co-existing apatite is barren of REE. Geochemical analyses of these rocks detected only minor enrichments of REE with the exception of Ce which showed considerable enrichment.

4.4 Genesis.

Mineralogy of alteration gives the best indication of genetic processes. Change in bulk chemistry between altered and unaltered rocks is shown in figure 4.1. To accomplish significant transfer of Si, Na and Mg, even locally, requires a high fluid : rock ratio. Both alteration types require copious quantities of CO₂ which could be supplied by water-graphite reactions or skarnification of limestones. Either of these mechanisms is compatible with property geology. Xenotime and monazite are likely unstable at greenschist facies metamorphism (Overstreet, 1960) and are characteristically found in rocks formed in the presence of high fluid activity such as pegmatites, gneisses and migmatites. Partitioning of heavy REE into xenotime and no coexisting apatite is a feature noted in vapour dominated, hydrothermal systems (Vaslov, 1966).

The similarity in age (and chemistry) of alteration on the property area with that of Galore Creek suggests a genetic affinity with syenite or monzonite intrusives. Early silica-

potassic alteration and mineralization may have arisen from localized, plutonically induced, metamorphic fluids; particularly where fluids may have been ponded by impermeable greenstones. Retrograde boiling and related volume expansion within the intrusion could cause extensive hydraulic fracturing and release of both metamorphic and magmatic fluids causing carbonate-oxide alteration, carbonate sulphide veins and quartz breccia veins.

5. SUMMARY AND CONCLUSIONS

Paleozoic rocks of the BJ claim area consist of mafic to acid volcanics and pyroclastics erupted in an ocean island, plate tectonic setting. These volcanics and related sediments merged with a subduction zone (Cache Creek Group) and a volcanic arc (Triassic volcanics and intrusives) to form a composite terrane during Triassic time. This composite terrane was accreted to the continent margin during the mid-Jurassic and caused widespread orogeny.

Structural and chronological data demonstrate that alteration and mineralization of BJ group rocks began during, or prior to, the onset of deformation and terminated after deformation. Regional greenschist facies metamorphism may have occurred during or prior to, deformational events, but is overprinted by post deformational metamorphism. Regionally, sharp transitions in the degree of deformation and metamorphism of similar aged rocks and coincident age determinations for alteration and mineralization with plutonic events strongly suggest that dynamothermal metamorphism, alteration, and mineralization is related to mid-Jurassic intrusives.

Tectonic overpressure caused during terrane accretion and/or emplacement of plutons caused locally steep geothermal gradients to occur. These gradients developed a hydrothermal system, either by metamorphic dewatering or by utilizing meteoric water modified by metamorphic reactions, which is characterized by high CO_2 content, high $\text{K}^+:\text{Na}^+$ ratios, and low pH. This hydrothermal system, possibly aided by ponding beneath

impermeable greenstone sills, caused widespread silica-potassic alteration and secretion of quartz-pyrite veins. Silica potassic alteration zones became the locus for much of the subsequent deformation during forceful emplacement of intrusives. Retrograde boiling and related volume expansion of magma induced hydraulic fracturing and consequent escape of volatile fluids caused carbonate-oxide alteration and mineralization. Self-sealing vents caused repetitive fracturing and mineralization.

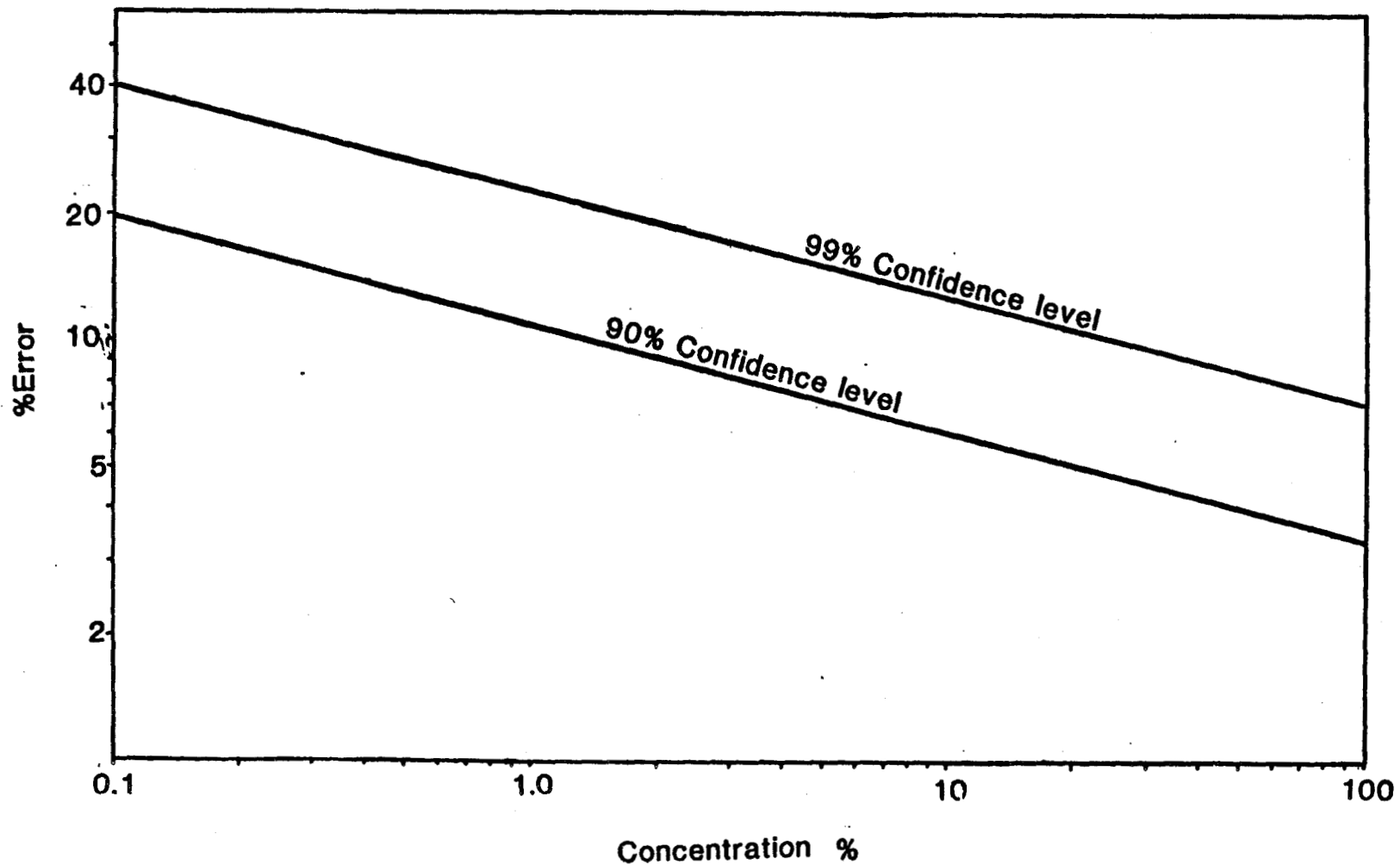
Widespread, weakly mineralized carbonate-oxide alteration most likely accounts for geochemical anomalies. However, higher grade quartz and manganese-siderite-sulphide veins are better exploration targets. Gold occurs as tiny free grains in both quartz and carbonate gangues and associated with tetrahedrite and tellurides. Gold distribution is erratic but tetrahedrite, galena and sphalerite are good indicator minerals.

REFERENCES

- Allens, D.G., Panteleyev, A., Armstrong, A.T., 1976
Galore Creek, in Porphyry Deposits of the Canadian Cordillera. C.I.M. Spec. Vol. 15, p.402.
- Amlı, R., 1975 Mineralogy and Rare Earth Geochemistry of Apatite and Xenotime from Gloserheta Pegmatite, Froland, Norway. Am. Mineralogist, Vol. 60. pp 607-620.
- Berman, R., 1977 The Coquihalla Volcanic Complex, S.W.B.C. Unpub. M.Sc. Thesis, U.B.C.
- Boyle, R. W., 1979 The Geochemistry of Gold and its Deposits. G.S.C. Bull. 280.
- Cox, K.G., Bell, J.D. and Pankhurst, R.J., 1979.
The Interpretation of Igneous Rocks. George, Allen and Unwin Pub. London.
- Currie, K.L. and Ferguson, J., 1971.
A study of Fenitization around the Alkaline Carbonatite complex at Callender Bay, Ontario, Canada. Can. J. Earth Sci. Vol. 8, pp 498-517.
- Finlow-Bates, T and Stumpf, E.F., 1981. The Behaviour of So-called Immobile Elements in Hydrothermally altered rocks Associated with Volcanogenic Submarine-Exhalative ore Deposits. Mineralium Deposita Vol.16, pp. 319-328.
- Floyd, P.A. and Winchester, J.A., 1978.
Identification and Discrimination of Altered and Metamorphosed Volcanic Rocks Using Immobile Elements. Chem. Geol. Vol. 21, pp. 291-306.
- Garcia, M.O., 1978, Criteria for the Identification of Ancient Volcanic Arcs. Earth-Sci. Reviews, Vol.14, pp 147-166.
- Holm, P.E., 1982 Non-Recognition of Continental Tholeiites using the Ti-Y-Zr Diagram. Contribs. to Min. and Petr. Vol. 79, No. 3, p.308.
- Irvine, T.N. and Baragar, W.R.A., 1971.
A guide to the Chemical Classification of Volcanic Rocks. Can. J. Earth Sci. Vol.8, pp.523-545.
- Kerrick, R. and Hodder, R.W., 1982
Archean Lodegold and Base Metal Deposits: Chemical Evidence for Metal Fractionation into Independent Hydrothermal Reservoirs. C.I.M. Special Vol. 24 pp 144-160

- Monger, J. W., 1977, Upper Paleozoic Rocks of the Western Cordillera and their Bearing on Cordilleran Evolution. Can. J. Earth Sci. Vol. 14, pp 1832-1859.
- Monter, J.W., Price, R. A. and Templeman-Kluit, D.J., 1981
Tectonic Accretion and the Origin of the Two Major Metamorphic and Plutonic Welts in the Canadian Cordillera. Can. J. Earth Sci.
- Ohomoto, H., and Kerrich, D., 1977.
Devolitization Equilibria in Graphitic Systems. Am. J. Sc. Vol. 277, pp. 1013-1044.
- Overstreet, W. C., 1960. Metamorphic Grade and Abundance of ThO₂ in Monazite. USGS Prof. Paper 400-B. pp.55-57
- Panteleyev, A., 1973. B.C.D.M. Reports
- Pearce, J.A., and Cann, J.R., 1975.
Tectonic Setting of Volcanic Rocks Determined using Trace Element Analyses. Earth and Planetary Sci. Letters, Vol. 19. pp 290-300.
- Thompson, M. and Howarth, R. J., 1976.
Duplicate Analysis in Geochemical Practice Analyst, 101. pp 690-709.
- Thompson, M. and Howarth, R. J., 1978.
A new approach to the Estimate of Analytical Precision. J. Geochem. Expl., Vol. 9, pp. 23-30.
- White, W.H., Harakal, J.E. and Carter, N.L., 1968.
Potassium-Argon Ages of Some Ore Deposits in British Columbia.
- Winkler, H., 1976. Petrogenesis of Metamorphic Rocks. Springer-Verlag Pub. New York.
- Van Der Heyden, P., 1982.
Tectonic and Stratigraphic Relations Between the Coast Plutonic Complex and Intermontane Belt, West Central B. C., Unpub. M.Sc. Thesis U.B.C.
- Vlasov, K.A., 1966. Geochemistry of Rare Elements. Academy of Sciences, USSR. Isreal Program for Scientific Translations Ltd.

APPEND. I



Relative error (precision) as a function of concentration at the 90% and 99% confidence levels. Graph is applicable to trace elements with the exception of Ce, Nd and Rb, which have appreciable error over the range of 1 to 1,000 ppm. The probability of a single analysis plotting outside the confidence limits, even when the entire batch is within limits, is given by the binomial distribution, e.g. in a batch of 20 replicate analyses, the probability that one pair will have greater error than that shown is 0.82 for the 90% level, and 0.04 for the 99% level. Two out of twenty samples having greater error than the 90% confidence level is 0.36 and therefore indicates that the precision of the batch is less than that shown.

CORRELATION MATRIX

	SI	AL	FE	MG	CA	NA	K	TI	MN	P	NI
SI	1.0000										
AL	-0.5913	1.0000									
FE	-0.8445	0.3554	1.0000								
MG	-0.8515	0.4005	0.5806	1.0000							
CA	-0.5348	0.2344	0.1814	0.4366	1.0000						
NA	-0.5059	0.2911	0.1427	0.7246	0.3628	1.0000					
K	0.3039	0.1992	-0.1661	-0.5235	-0.3142	-0.6345	1.0000				
TI	-0.7460	0.3875	0.7582	0.6109	0.1705	0.2248	-0.3211	1.0000			
MN	0.0389	-0.2530	0.2813	-0.2266	-0.2613	-0.2942	0.1228	-0.0983	1.0000		
P	-0.7563	0.3952	0.6683	0.6834	0.2530	0.4526	-0.3697	0.8597	-0.2436	1.0000	
NI	-0.0007	-0.0588	-0.2446	0.1715	0.3436	0.3383	-0.2409	-0.2385	-0.1150	-0.2521	1.0000
CR	0.0290	-0.1487	-0.2858	0.0766	0.5236	0.2691	-0.2417	-0.3294	-0.0514	-0.3061	0.8688
V	-0.8390	0.4640	0.8170	0.6949	0.2555	0.3906	-0.2770	0.8035	-0.1762	0.8637	-0.3351
CE	0.1843	-0.2726	0.1241	-0.4928	-0.0816	-0.5191	0.3229	-0.2587	0.8148	-0.3376	-0.0320
ND	-0.2199	0.0067	0.2981	0.1343	-0.0906	0.0138	-0.0742	0.4452	0.2595	0.4544	-0.2990
NB	-0.2923	0.4679	0.3760	0.1660	-0.2753	0.1091	-0.0124	0.3844	0.0991	0.4488	-0.4988
ZR	-0.0609	0.0607	0.2294	-0.0488	-0.2526	-0.2059	-0.0625	0.3829	0.1700	0.3658	-0.6627
Y	0.0446	0.3368	-0.0123	-0.1341	-0.2043	0.0955	0.1034	-0.1575	-0.2649	0.1288	-0.0874
RB	0.2758	0.1697	-0.2510	-0.2812	-0.2926	-0.3947	0.7096	-0.3722	0.0351	-0.3545	0.0215
SR	-0.2220	-0.1740	0.1249	0.2059	0.4072	0.3486	-0.3091	0.1157	-0.2491	0.3147	0.1932

CORRELATION MATRIX

	CR	V	CE	ND	NB	ZR	Y	RB	SR
CR	1.0000								
V	-0.3532	1.0000							
CE	0.1076	-0.3183	1.0000						
ND	-0.2234	0.3175	0.2214	1.0000					
NB	-0.5346	0.4576	-0.2004	0.2081	1.0000				
ZR	-0.6762	0.3146	-0.0270	0.5273	0.6766	1.0000			
Y	-0.1853	0.1488	-0.0373	-0.0383	0.2869	0.0719	1.0000		
RB	-0.1056	-0.4091	0.2576	-0.1976	-0.2913	-0.3487	0.1819	1.0000	
SR	0.1992	0.2355	-0.0585	0.3593	-0.2386	-0.0038	0.1711	-0.3380	1.0000

Appendix II: Correlation matrix for major and trace elements based on 21 samples. Values of $|r| \geq 0.5$ are significant.

APPENDIX IV
STATEMENT OF COSTS*

1. Petrology			
Polished thin sections 40 @ \$10		\$ 400	
SEM/EDS 30 hrs. @ \$15/hour		<u>450</u>	\$ 850
2. Geochemistry			
XRF 60 hrs. @ \$10/hour		600	
XRD 10 hrs. @ \$5/hour		50	
Computing time		150	
Gold analyses 30 @ \$8.00		<u>240</u>	1,040
3. Geochronology			
13 Rb/Sr determinations @ \$110		1,430	
1 k/Ar Age @ \$375		<u>375</u>	<u>1,805</u>
			\$ 3,695
Report Preparation			<u>\$ 2,300</u>
			<u>\$ 5,995</u>

*all costs reflect internal costs at U.B.C.

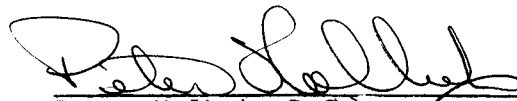
APPENDIX V

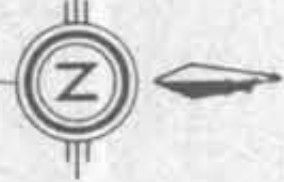
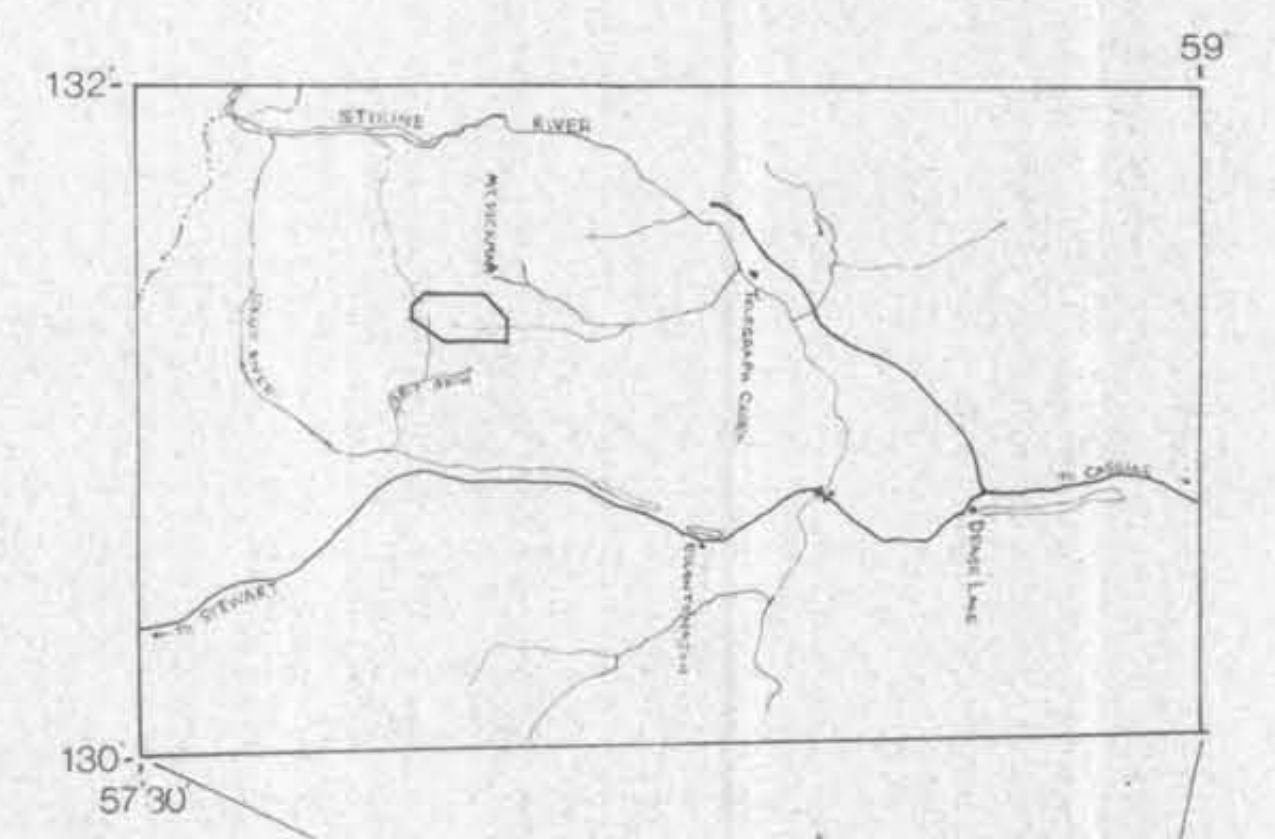
CERTIFICATE OF QUALIFICATIONS

PETER HOLBEK, B.Sc.

I hereby certify that:

1. I graduated from the University of British Columbia in 1980 with a B.Sc.(Hons.) Degree in Geological Sciences;
2. I am presently completing an M.Sc. degree in Geology at the University of British Columbia;
3. I have worked as a geologist or assistant for the past seven field seasons;
4. The work described herein was done under my direct supervision.


Peter Holbek, B.Sc.



TECK EXPLORATIONS LTD.
 B J GROUP
 CLAIMS, SAMPLE LOCATIONS

186 ● SAMPLE LOCATION
 ■■■■■ MINERALIZATION

GEOLOGICAL BRANCH
 ASSESSMENT REPORT

10,917